

**EVALUATING WHEELCHAIRS FOR POTENTIAL  
USE AS AIRCRAFT SEATING: STATIC AND  
DYNAMIC FRONTAL TEST CONDITIONS  
(INTERIM PROJECT REPORT)**

---

**KATHLEEN D. KLINICH, NICHOLE R. ORTON,  
KYLE BOYLE, TYLER VALLIER, BRIAN EBY, JENNIFER  
BISHOP, GARY WEISSEL, MIRIAM A. MANARY**

## **DISCLAIMER**

This research was sponsored by the National Institute on Disability, Independent Living, and Rehabilitation Research (NIDILRR). The opinions, findings, and conclusions expressed in this publication are those of the authors and not necessarily those of NIDILRR, the Department of Transportation (DOT), or the Federal Aviation Administration (FAA). If trade or manufacturers' names or products are mentioned, it is because they are considered essential to the object of the publication and should not be construed as an endorsement.

## **ACKNOWLEDGEMENTS**

We would like to thank the following individuals for their expertise and guidance on this project.

Brian Bard, NIDILRR

Anjali Forber-Pratt, NIDILRR

Kelly Buckland, DOT

Jeff Gardin, FAA

David Moorcroft, FAA

Joseph Pelletiere, FAA

Stacey Zinke, FAA

## Technical Report Documentation Page

1. Report No. UMTRI-2024-01	2. Government Accession No.	3. Recipient's Catalog No.	
4. Title and Subtitle Evaluating Wheelchairs for Potential Use as Aircraft Seating: Static and Dynamic Frontal Test Conditions (Interim Project Report)		5. Report Date February 2024	
		6. Performing Organization Code	
7. Author(s) Kathleen D. Klinich, Nichole R. Orton, Kyle J. Boyle, Tyler Vallier, Brian Eby, Jennifer Bishop, Gary Weissel, Miriam A. Manary		8. Performing Organization Report No. UMTRI-2024-01	
9. Performing Organization Name and Address University of Michigan Transportation Research Institute 2901 Baxter Rd. Ann Arbor, MI 48109		10. Work Unit No. (TRAIS)	
		11. Contract or Grant No. 90IFRE0072-01-00	
12. Sponsoring Agency Name National Institute on Disability, Independent Living, and Rehabilitation Research (NIDILRR)		13. Type of Report and Period Covered Interim 9-22 to 12-23	
		14. Sponsoring Agency Code	
15. Supplementary Notes			
16. Abstract <p>For this project, we hypothesized that wheelchairs meeting the voluntary standards for vehicle crashworthiness (RESNA WC19) would be able to pass the FAA crashworthiness standards for aircraft seating. In all tests, wheelchairs were secured using surrogate 4-point strap tiedowns in the geometry specified by WC19. Seven wheelchairs representing a range of wheelchair designs were tested. For the static tests, two manual wheelchairs met requirements, but applying the entire load through the seat caused damage to the power wheelchairs. Discussion with FAA experts suggested an alternative interpretation of the standard to allow splitting the load between the seat and base for future static trials. For the dynamic frontal testing, modeling was used to demonstrate the suitability of using the trapezoidal pulse achieved with the UMTRI sled produced rather than the typical triangular shaped FAA pulse, as well as the minimal effect of simulating pitch and roll with the test fixture because of the non-rigid 4-point strap tiedowns. In the first two dynamic frontal tests, the left front caster wheel broke. Subsequent tests of five wheelchair models using an additional aircraft-mounted lap belt (suggested by FAA experts) were successful. Based on these results, it may be feasible for people to use their own wheelchairs on aircraft if they use WC19 wheelchairs secured to the aircraft with 4-point strap tiedown systems, supplemented by an occupant lap belt anchored to the aircraft. Additional work is needed to interpret requirements of static tests for heavier power wheelchairs, conduct testing on different wheelchair products, and test wheelchairs according to the dynamic vertical aircraft seating requirements.</p>			
17. Key Words Wheelchairs, aircraft, static, frontal, FAA		18. Distribution Statement	
19 Security Classif. (of this report) Unclassified	20. Security Classif. (of this page) Unclassified	21 No. of Pages 70	22. Price

## Contents

<i>List of Figures</i>	v
<i>List of Tables</i>	viii
<i>Introduction</i>	1
<b>Importance of the Problem</b>	1
<b>Current Relevant Standards and Guidelines</b>	3
<b>Wheelchair Transportation Safety</b>	5
<b>Project Objective</b>	9
<i>Adapting FAA Test Conditions for Wheelchairs</i>	10
<b>Attachment Conditions</b>	10
<b>Wheelchair Station Location Potential Contact with Bulkhead</b>	17
<b>ATD Selection</b>	20
<b>Sled Pulse</b>	21
<b>Yaw, Pitch, and Roll</b>	25
<b>Wheelchair selection</b>	28
<i>Static testing</i>	29
<b>Methods</b>	29
<b>Results</b>	34
<i>Dynamic Frontal Testing</i>	45
<b>Methods</b>	45
<b>Results</b>	47
<i>Discussion</i>	57
<i>Summary and Conclusions</i>	59
<i>Ongoing Work</i>	60
<i>Bibliography</i>	61
<i>Appendix A. Additional Dynamic Testing Results</i>	64
<i>Appendix B. Draft Test Procedure for Wheelchairs Under Frontal Aircraft Seating Conditions</i>	67
<b>Introduction</b>	68
<b>Wheelchair Test Methods</b>	68
<b>Wheelchair Performance Criteria</b>	69

## List of Figures

Figure 1. Examples of wheelchair engaged with docking system mounted to vehicle floor (left) and example of mating hardware with low ground clearance (right). .....	6
Figure 2. Example of a wheelchair secured by 4-pt strap tiedown system.....	6
Figure 3. Rear-facing wheelchair passenger station (left) and Q'Straint Quantum automated docking system (right). .....	7
Figure 4. Examples of prototype UDIG-compatible attachments for manual wheelchair (left), power wheelchair (right), and UDIG-compatible vehicle anchor (right). .....	7
Figure 5. Crash-tested wheelchair restraints.....	8
Figure 6. Surrogate wheelchair tiedown (left), surrogate wheelchair (center), and surrogate wheelchair base (right).....	9
Figure 7. Illustration of best practice recommendations for securing wheelchairs with 4-point strap tiedowns. ....	10
Figure 8. Fixture used to check that wheelchair securement points are in recommended zone. ..	11
Figure 9. Comparison of kinematics under frontal loading conditions for recommended (red) and vertical (blue) tiedown geometry at 0, 60, 120, 180, and 240 ms.....	13
Figure 10. Comparison of kinematics under vertical loading conditions for recommended (red) and vertical (blue) tiedown geometry at 0, 60, 120, 180, and 240 ms.....	14
Figure 11. Comparison of tiedown loads under frontal loading for recommended (red) and vertical (blue) tiedown geometries.....	15
Figure 12. Comparison of tiedown loads under vertical loading for recommended (red) and vertical (blue) tiedown geometries.....	16
Figure 13. Comparison of lap belt loads for frontal (left) and vertical (right) for recommended (red) and vertical (blue) tiedown geometries. ....	16
Figure 14. Rear (left) and front (right) SWTORS used to secure wheelchairs during WC19 testing.....	17
Figure 15. Key landmarks on a manual wheelchair (left) and power wheelchair (right). .....	18
Figure 16. Variation in bight location of 75 wheelchairs, when rearmost point of wheelchair is the origin. ....	18
Figure 17. Suggested geometry with tiedowns located at rear of station, bulkhead located 152 cm (60 in) forward, indicating that the average SRP would be rearward of the 107 cm (42 in) arc requiring representation of bulkhead during testing. ....	19

Figure 18. Alternative geometry with SRP located 107 cm (42 in) from bulkhead, showing there may be insufficient space to secure longer wheelchairs appropriately. ....	20
Figure 19. Comparison of ideal and UMTRI versions of the FAA horizontal pulse.....	21
Figure 20. Comparison of kinematics between the UMTRI and triangular versions of the FAA pulse. ....	22
Figure 21. Comparison of head and pelvis excursions for UMTRI pulse (red) and triangular pulse (blue). ....	23
Figure 22. Comparison of resultant head, chest and pelvis accelerations (top row) and ATD-to-seat force, WC-to-floor-force, and seatbelt-to-ATD contact force between UMTRI (red) and triangular (blue) frontal FAA pulse conditions. ....	24
Figure 23. Comparison of peak lumbar force between UMTRI and triangular frontal FAA pulse conditions. ....	24
Figure 24. Simulations showing the effect on ATD and wheelchair kinematics with and without prescribed floor deformation (gold=fixed, purple=deformed). ....	26
Figure 25. Simulations showing small differences in ATD-to-seat force, WC-to-floor force, peak head X excursion, and pelvis X excursion with and without prescribed floor deformation (gold=fixed, purple=deformed). ....	27
Figure 26. Example setup for frontal static pull test of QE2. ....	30
Figure 27. Example setup for rear static pull test of TLZ. ....	30
Figure 28. Example setup for lateral static pull test of JCS. ....	31
Figure 29. Examples of upward pull test of SQ700 (left) using winch mounted to ceiling beam, and downward pull test of KMC5 (right ) using sam overhead winch and pulleys to apply downward load. ....	31
Figure 30. Illustration of deformation using pre- and post-test 3D scans of wheelchairs. ....	33
Figure 31. Photos of peak rear static loading for SWCB (upper left), TLZ (upper right), KMC5 (middle left), JCS (middle right), QE2 (lower left), and SQ710 (lower right.) ....	35
Figure 32. Photos of peak downward static loading for SWCB (upper left), TLZ (upper right), KMC5 (middle left), JCS (middle right), QE2 (lower left), and SQ710 (lower right.) ....	36
Figure 33. Photos of peak upward static loading for SWCB (upper left), TLZ (upper right), KMC5 (middle left), JCS (middle right), QE2 (lower left), and SQ710 (lower right.) ....	37
Figure 34. Closeup photo of JCS seat detached from base after upward loading test. ....	38
Figure 35. Photos of peak lateral static loading for SWCB (upper left), TLZ (upper right), KMC5 (middle left), JCS (middle right), QE2 (lower left), and SQ710 (lower right.) ....	38
Figure 36. Damage to QE2 sustained during lateral static testing. ....	39

Figure 37. Damage to JCS sustained during lateral static testing .....	39
Figure 38. Damage to SQ710 sustained during lateral static testing .....	39
Figure 39. Photos of peak frontal static loading for SWCB (upper left), TLZ (upper right), KMC5 (middle left), JCS (middle right), QE2 (lower left), and SQ710 (lower right.) .....	40
Figure 40. Damage to QE2 sustained during lateral static testing .....	40
Figure 41. Damage to SQ710 sustained during lateral static testing .....	41
Figure 42. Damage to JCS sustained during lateral static testing .....	41
Figure 43. Static test results for TLZ .....	42
Figure 44. Static test results for KMC5 .....	42
Figure 45. Static test results for QE2 .....	43
Figure 46. Static test results for SQ710 .....	43
Figure 47. Static test results for JCS .....	44
Figure 48. Example of ATD secured by both wheelchair-anchored lap belt and vehicle-anchored lap belt .....	47
Figure 49. Sequence of closeup images from left video showing fracture of left front caster wheel .....	47
Figure 50. FEM results with KMC5 showing effective plastic strain distribution under UMTRI (left) and FAA (right) pulses .....	48
Figure 51. Average sled accelerations from all tests .....	49
Figure 52. Sled change in velocity from all tests .....	49
Figure 53. Lap belt load from all frontal tests .....	50
Figure 54. Rear tiedown loads from all frontal tests .....	51
Figure 55. Head resultant acceleration prior to head-to-leg contact from all frontal tests .....	52
Figure 56. Lumbar axial force from all frontal tests .....	53
Figure 57. ATD head path relative to the wheelchair seat junction from all frontal tests .....	54
Figure 58. Example sideview kinematics under frontal dynamic loading for CVS_0 .....	55
Figure 59. Example overhead kinematics under frontal dynamic loading for CVS_0 .....	56
Figure 60. Complete head resultant acceleration from all frontal tests .....	65
Figure 61. Chest resultant acceleration from all frontal tests .....	65
Figure 62. Pelvis resultant acceleration from all frontal tests .....	66
Figure 63. Upper neck axial force from all frontal tests .....	66

## List of Tables

Table 1. Summary of first set of wheelchairs purchased for testing .....	28
Table 2. Wheelchair masses and target applied load for each static test direction. ....	32
Table 3. Dynamic frontal test matrix. ....	46



# Introduction

## Importance of the Problem

Access to transportation is essential for employment, education, healthcare services, and other activities of daily living. According to the American Community Survey (ACS), an annual survey conducted by the United States (US) Census Bureau, the overall percentage of people with a disability in the US in 2017 was 12.7% [1]. Among the six categories of disabilities identified by the ACS, the highest prevalence across all ages was the 6.9% reported as having an ambulatory disability, which increases with age.

Approximately 5.5 million people in the US use wheelchairs, but they are not currently allowed to use them as seats on aircraft. This can be a deterrent to people whose medical needs, such as periodic pressure relief and postural support, are met by the specialized features on their wheelchairs [2]. Among those that transfer to airline seating, many report instances of their wheelchairs being damaged during transport in the luggage compartment, as well as discomfort, injury, and social stigma experienced while transferring to a standard aircraft seat. In a public listening session sponsored by the US Access Board in Fall 2022, many participants reported being dropped during transfer to the aircraft seat. In a recent worst-case scenario, a disability activist died from injuries sustained when she was unable to use her custom wheelchair that was damaged during transport in the aircraft's cargo hold [3].

The Americans with Disabilities Act of 1990 [4] and the ensuing American with Disabilities Act Accessibility Guidelines (ADAAG) issued by the US Access Board [5] are intended to ensure that public spaces, public communication, and public transportation are usable and accessible to people with disabilities. This work incorporated many ideas from the foundational efforts of the Rehabilitation Act, Fair Housing Amendments Act, Architectural Barriers Act, and related work. The US Department of Transportation (DOT) and Department of Justice (DOJ) interpret the ADAAG to write enforceable standards that are consistent with, and meet at least the minimum specifications of, the Access Board guidelines. While airports are held to these accessibility standards, aircraft are currently exempt from the requirements and the accommodations found in other forms of public transportation. When the ADA was introduced, the space and safety requirements for aircraft were considered too challenging to require accommodations for personal wheelchair use. However, the success of accommodating wheelchair users in other transportation modes since then has motivated Congress in 2018 to direct the FAA to revisit the topic.

Unlike most other forms of public transportation, aircraft do not offer a means of allowing a person using a wheelchair to remain seated in their own device during a trip. In 2018, the FAA Reauthorization Act directed the US Access Board to examine the feasibility of installing wheelchair seating stations on aircraft. The Access Board commissioned the National Academy of Sciences (NAS) to appoint a 12-member committee of experts to examine the issue [2]. A member of the University of Michigan Transportation Research Institute (UMTRI)'s project team, Miriam Manary, served as one of the twelve members of the committee. Gary Weissel, an aircraft consultant advising our project, was also a member of the committee.

As part of the information gathering step, the NAS committee heard testimony from stakeholders that represented government agencies, wheelchair manufacturers, aircraft manufacturers, flight attendants, disability advocates, airlines, an airline industry trade association, adaptive equipment manufacturers, and consumer organizations. Many of the participants were wheelchair users who had personally experienced airline transportation challenges, injuries, and lost opportunities due to lack of accommodations for mobility disabilities in aircraft.

The three main technical issues examined in the feasibility study were whether there was sufficient doorway clearance and interior space to allow maneuvering and securement of most wheelchairs, whether an airplane floor and structure could withstand the loadings of a secured power wheelchair, and whether a secured wheelchair could meet the regulated safety performance specifications required for standard aircraft seats.

The committee determined that most transport category aircraft have sufficient door and entry area clearances (with some potential modifications) to accommodate most wheelchairs. Due to current aircraft aisle widths, the committee determined that the most likely location of a wheelchair securement area would be adjacent to an aircraft entry door. They evaluated one potential concept that included removing two rows of seats in the cabin to provide room for a wheelchair securement system. This concept would provide sufficient space to locate a feasible wheelchair station with enough room to maneuver and secure the wheelchair, and allow adequate clearance to avoid potentially injurious head contacts of the wheelchair user and other passengers. In addition, the two rows of removed seats (and the passengers who would use those seats) would be of similar mass to a heavy power wheelchair and its occupant, indicating that the existing floor strength should be sufficient to allow docking of a power wheelchair.

Regarding wheelchair securement, the committee noted that wheelchairs meeting voluntary WC19 crashworthiness standards for motor-vehicle use have four dedicated securement brackets for attaching tiedown straps in standardized locations, and have the option for a crashworthy lap belt. These features were considered suitable as a standardized interface for securing wheelchairs on aircraft. In addition, the WC19 frontal crashworthiness test was considered similar to but more severe than the FAA frontal crashworthiness test required for aircraft seats. However, the ability of WC19 wheelchairs to pass the FAA vertical crashworthiness tests, as well as flammability tests, is uncertain.

While the committee's main goal was to address technical issues, they also provided an overview of potential operational issues. Locating the wheelchair station near the main boarding door would allow an equitable level of service to other passengers and avoid extensive changes to aircraft standard aisle widths that would not be feasible. They noted that allowing passengers in wheelchairs will require changes in reservation systems, procedures for validating wheelchair boarding eligibility, access to power during flight to operate power wheelchairs (specifically for recline / pressure relief operations), and providing passenger assistance. A potential concern was whether wheelchair users could become stranded en route if scheduling problems result in a connecting flight plane not having a wheelchair station. They noted that the demand for wheelchair seating stations on planes is currently unknown, as no data are available on potential passengers who do not currently fly but who would if staying seated in their own wheelchair was an option.

The committee concluded that providing wheelchair seating stations on aircraft should be technically feasible. They recommended a study to assess demand for wheelchair stations among potential customers.

The report also suggested additional research to determine whether wheelchairs could meet the existing Federal Aviation Administration (FAA) crashworthiness requirements for aircraft seats. These consist of a dynamic 16 g frontal impact, with the seat angled 10 degrees to the left or right, as well as a 14 g dynamic test with the seat positioned 60 degrees relative to horizontal to assess crashworthiness to vertical loading, and static pull tests in several directions.

### **Current Relevant Standards and Guidelines**

#### *RESNA & ISO Wheelchair Transportation Safety Standards*

RESNA has a suite of standards contained in four volumes that establish ways to measure, define, and test wheelchairs and wheelchair components. The RESNA voluntary standards are recognized by the American National Standards Institute (ANSI) and include Volume 4 Section 10 Wheelchair Containment and Occupant Retention Systems for Large Accessible Transit Vehicles (WC10) [6], Section 18 Wheelchair Tiedowns and Occupant Restraint Systems (WC18) [7], Section 19 Wheelchairs used as Seats in Motor Vehicles (WC19)[8], and Section 20 Wheelchair Seating (WC20) [9]. A set of similarly-intentioned voluntary standards exist for global use within the International Organization for Standardization (ISO) that are developed and maintained by international experts through four working groups under Technical Committee 173, Subcommittee 1. These ISO standards overlap significantly with the US national standards, with standards 10865-1, 10542-1, 7176-19, 16840-4, being international versions of WC10, WC18, WC19, and WC20, respectively. Standards WC10, 10865-1 and 10865-2 specifically address wheelchair spaces in large accessible transit vehicles (LATVs) and place a high emphasis on independence in an environment that does not require a high level of crashworthiness. A key difference between WC19 and ISO 7176-19 is that only WC19 requires the option for a wheelchair-mounted crashworthy lap belt.

#### *Code of Federal Regulations Title 14 Part 25: Airworthiness Standards: Transport Category Airplanes*

Requirements for transport category aircraft interiors are prescribed in Title 14 Part 25 of the Code of Federal Regulation (14 CFR 25). Sections 25.561 and 25.562, under Emergency Landing Conditions, address the crashworthiness and testing of seating.

Section 25.561 contains the original crashworthiness requirements that are accomplished with static pull testing of the seat in five directions: upward, forward, laterally, downward, and rearward. Each direction has a different pull force specified in g: 3 g upward pull, 9 g forward pull, 4 g lateral pull, 6 g downward pull and 1.5 g rearward pull. The load level for the pull is determined by adding the mass of the seat to the mass of a 170 lb midsize male occupant and then multiplying this total mass by the g level and scale factor needed. To comply with requirements, the seat cannot experience structural failure when pulled in the various directions, and cannot deform to an extent that it would interfere with egress.

Section 25.562 was added in the late 1980s, and includes two dynamic testing scenarios intended to simulate the forces of a crash. Section 25.562 applies to most newer models of aircraft. For these tests, an instrumented midsize male anthropomorphic test device (ATD), or crash test dummy, is used to represent a typical occupant restrained by the provided lap belt. The regulation specifies a vertical crash scenario that tests the seat's ability to remain intact, keep the occupant seated, retain items of mass, and limit vertical loads through the ATD's spine during a crash landing. The required pulse for this is 14 g deceleration achieved within 80 ms with a change in velocity of at least 38.4 km/h. A second, primarily frontal, impact test is conducted with the seat yawed at 10 degrees to the left or right relative to the impact direction. The frontal pulse requirements are 16 g achieved within 90 ms providing a delta V of at least 48.2 km/hr. The frontal pulse also has requirements to simulate floor deformation. This test checks the seat's dynamic strength, as well as the risk of occupant injury from interaction with interior components, such as the head striking other seats or barriers directly adjacent to the seating area. Seats are not allowed to deform to the extent that they would block egress during exit. The ATD is instrumented to measure head acceleration, as well as femur compressive loads, and the standard establishes allowable limits on the injury risk measures from the ATD. The head injury criterion (HIC) value cannot exceed 1000, the pelvic vertical compression must not exceed 1500 lbf, and the femur load must not exceed 2250 lbf.

In addition to seat crashworthiness, CFR 25.562 also requires that "items of mass" cannot shift or break free to create a projectile hazard in the occupant compartment. For seating, this requirement is met by assuring that no parts (with significant weight) of the seating shift or come off during the static or dynamic testing.

In addition to the standard, FAA Advisory Circular 25.562-1B, Dynamic Evaluation of Seat Restraint Systems and Occupant Protection on Transport Airplanes/with Change 1 (FAA 1989), provides guidance and details regarding acceptable methods of testing to the standard.

#### *SAE Aerospace Recommended Practices and Standards*

SAE Aerospace Recommended Practice ARP6909 (November 2020) "Methods for Determining the Seat Reference Point (SRP) and the Buttock Reference Point (BRP) for Seats in Transport Aircraft, Civil Rotorcraft, and General Aviation Aircraft" defines acceptable methods for identifying the SRP and BRP in aircraft seats. The SRP is essentially the intersection of the seatback and seatpan with the ATD in the seat. The BRP "are the points on the bottom surface of the buttocks directly below each ischial tuberosity when sitting in the seat."

SAE Aerospace Standard AS8049D (November 2020), "Performance Standard for Seats in Civil Rotorcraft, Transport Aircraft, and General Aviation Aircraft" provides more specific details regarding how to test aircraft seats to meet FAA requirements [10]. AS8049 covers different types of aircraft categories; Seat Type A-T used in Transport Airplanes addressed in 14 CFR part 25 are relevant for the current project. Section 3.5 specifies methods for documenting permanent deformations after testing. Measurement of deformation in the forward direction usually tracks the forwardmost hard point of the seat. The seatpan cannot rotate more than 20 degrees pitch down or 35 degrees pitch up. The maximum lateral deformation is measured at a point above and

below a point 635 mm from the floor. The seatback cannot deform forward beyond the original seatpan fore-aft midpoint.

For the static loading tests, AS8049 expands upon the requirements in the FAA regulation. Static loads should be applied for at least 3 seconds without failure. Loads are applied through a body block, placed such the load is generally 270 mm above the SRP and 215 mm forward of the SRP.

Details are also provided for two dynamic test conditions. The ideal pulse shapes meeting the specifications of the standard is described as an isosceles triangle. The standard provides illustrations of how the floor deformation of  $\pm 10$  deg pitch and  $\pm 10$  deg roll can be implemented in a test fixture for different seating configurations. The standard also includes a seating procedure for placing the ATD in the seat. It lists the conditions when HIC should be calculated, which are limited to tests where the head strikes a forward seat or bulkhead representation, which is used when the distance from the SRP to the bulkhead is less than a typical front row clearance of 107 cm (42 in) [11].

### **Wheelchair Transportation Safety**

The scenario of a person who uses a wheelchair as a seat in a motor vehicle is not currently addressed in US federal motor vehicle safety standards (FMVSS). Wheelchairs are classified as medical devices and are regulated by the Federal Food and Drug Administration, which recognizes the RESNA Volume 4 standards but only applies them to products labelled for use as a seat in a motor vehicle. However, groups of stakeholders have used the precedents and crash protection principles of the FMVSS to establish voluntary industry standards to address this circumstance. As mentioned above in the Current Relevant Standards section, RESNA and ISO have voluntary test procedures for wheelchairs used as motor vehicle seats. Many of these standards and test procedures were developed at UMTRI through many series of sled tests, and current staff serve as experts on both RESNA and ISO working groups and/or committees that oversee revisions of these standards [12], [13], [14], [15], [16], [17], [18], [19], [20], [21], [22]. These standards currently include test protocols for frontal and rear impacts only.

To travel safely while seated in a wheelchair, a person needs to have a crash-tested wheelchair, a method to attach the wheelchair to the vehicle, and a method to restrain the occupant. WC19 [8] addresses the first point, by establishing design and performance requirements, and associated test methods, for wheelchairs related to their use as seats in vehicles. WC18 [7] addresses the latter points, with methods to evaluate Wheelchair Tiedown and Occupant Restraint System (WTORS) that consist of a system or device for securing wheelchairs, and a system of belts for restraining occupants seated in wheelchairs.

In motor vehicles, several different approaches for securing wheelchairs are used. For individuals who drive while seated in a wheelchair, the most common strategy involves customized hardware added to the bottom of wheelchair that docks into a securement system mounted on the vehicle floor. An example is shown in Figure 1. Good function of these systems depends on maintaining close alignment of the mating hardware to allow effective docking to occur between the wheelchair and vehicle. However, day-to-day differences in wheelchair tire pressure/wear or added wheelchair cargo can be enough to obstruct the process. Such systems are also customized for a particular pairing of a single user and a single private vehicle and would not be adaptable

for aircraft where one wheelchair space needs to accommodate many different people using wheelchairs.



Figure 1. Examples of wheelchair engaged with docking system mounted to vehicle floor (left) and example of mating hardware with low ground clearance (right).

For people traveling as passengers in modified vehicles or via public transportation, the most common method of securing the wheelchair to the vehicle is a 4-point strap tiedown system. An example is shown in Figure 2. With this tiedown method, four straps are anchored to reinforced points on the vehicle floor and hooked onto the wheelchair. This system allows a single WTORS to secure a wide range of wheelchair types and has been shown to be highly effective in the field. Wheelchairs that meet WC19 requirements have clearly marked, dedicated securement brackets for attaching the tiedowns. Although this system is the most common travel scenario for people who remain in their wheelchairs, few wheelchair users can independently secure their own wheelchairs with this technique, so a bus or paratransit driver typically secures the passengers' wheelchairs to the vehicle. While the dedicated securement brackets on a WC19 wheelchair simplifies the process, most people do not currently use WC19 wheelchairs, and the driver will hook the tiedowns on available wheelchair structures. On an aircraft, airport personnel or flight crews would need to assist with securement using 4-point strap tiedowns.

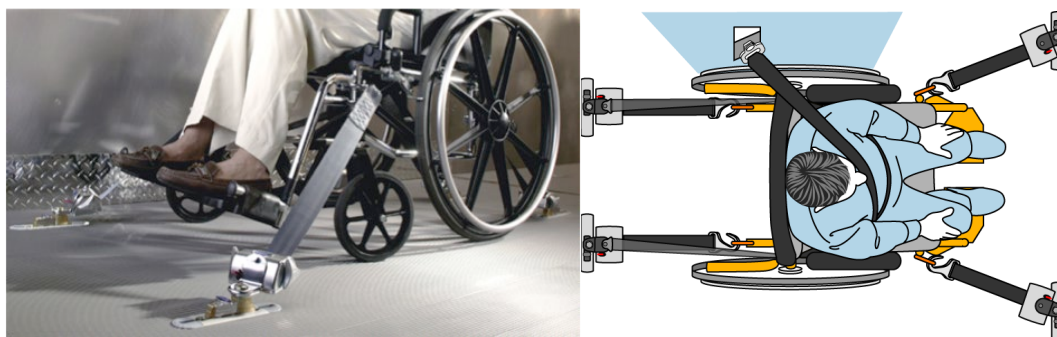


Figure 2. Example of a wheelchair secured by 4-pt strap tiedown system

ADA guidelines allow the use of rear-facing wheelchair passenger stations on large, heavy buses. Examples are shown in Figure 3. These offer a high level of independence on large accessible transit vehicles (LATVs), and provide wheelchair users with a similar level of protection as the other LATV passengers who are unrestrained in the bus seats and who are allowed to stand during vehicle travel. However, rear-facing stations are not robust enough to

pass the crash severity requirements for lighter, minivan-sized vehicles or aircraft when all items and people must be secured. Rear-facing wheelchair passenger stations have been deployed since 2005 in some major metropolitan bus systems, while the Q'Straint Quantum autonomous docking stations (an enhanced version of rear-facing station) have entered the market more recently. The NAS report indicated that these would not be viable securement method on aircraft.



Figure 3. Rear-facing wheelchair passenger station (left) and Q'Straint Quantum automated docking system (right).

The Universal Docking Interface Geometry (UDIG), shown in Figure 4 [23], is one proposed solution for making docking stations that can work in a public transportation setting where one wheelchair station must secure many types of wheelchairs. UDIG defines an interface geometry and interface location that can be the basis for design of docking stations and dockable wheelchairs. Specifications for UDIG geometry are included in informative and normative annexes of current wheelchair transportation safety standards in the US and internationally. For the wheelchair and anchors, as shown in Figure 4, the required UDIG elements are two, 22-mm diameter, 75-mm long, vertical tube-shaped features located on the lower rear of the wheelchair that are spaced 222 to 333 mm apart. These are located on the wheelchair so that the bottom of the tubes is 203 mm above the floor surface. This concept is akin to the standardization of trailer hitches that allow any semi-tractor driver to attach and tow any trailer.

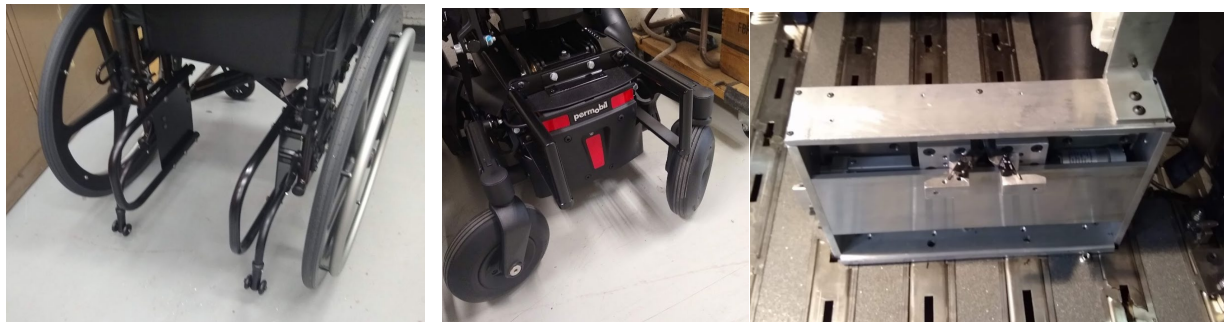


Figure 4. Examples of prototype UDIG-compatible attachments for manual wheelchair (left), power wheelchair (right), and UDIG-compatible vehicle anchor (right).

This geometry has been defined, prototyped, crash tested, and field tested[23], [24], [25], [26]. Several recent UMTRI studies [27], [28], [29], [30], [31] explored the UDIG approach as a possible solution to allow safe, independent use of automated vehicles (AVs) by people who remain seated in wheelchairs for travel. This project evaluated the system through computational modeling, dynamic testing in frontal and side impact conditions, and volunteer testing, and it seems a potentially feasible solution for AVs that could also work on aircraft. However, although the UDIG concept was introduced over 20 years ago, there are no commercially available products with UDIG hardware. The key barrier to implementation of the UDIG system is the voluntary nature of wheelchair safety standards; vehicles must be equipped with UDIG docking hardware and wheelchairs must be equipped with UDIG attachments hardware before the system is feasible.

People who drive while seated in their wheelchairs in private vehicles often use the lap and shoulder belt restraint system provided with the vehicle. However, in modified personal vehicles, the inboard buckle is often mounted to a stalk attached to the floor, as the original vehicle inboard buckle has been removed with the vehicle seat to create the wheelchair station. In addition, active safety features such as seatbelt pre-tensioners and occupant classification systems may be disconnected as part of the vehicle modification. Public transportation generally offers lap/shoulder belts attached to the bus that must be applied to the passenger by the driver. These seatbelt options often result in loose belt restraints or poorly placed belts due to interference with the wheelchair armrests and controls.

Because of challenges in donning belt systems, as well as issues with fit, an alternate solution is for the wheelchair to be equipped with a crash-tested lap belt. Examples are shown in Figure 5. These belt systems are currently offered on a limited number of wheelchairs and the option must be offered on a WC19 compliant wheelchair. The voluntary nature of wheelchair testing standards coupled with the increased expense of equipping wheelchairs with crash-tested belt restraints has limited their widespread deployment. However, the NAS report identified crash-tested lap belts attached to the wheelchair as the most viable option for using wheelchairs as aircraft seating. One of the key differences between WC19 and ISO 7176-19 is that the option for a wheelchair-anchored lap belt is only required by WC19.



Figure 5. Crash-tested wheelchair restraints



Creation of wheelchair transportation safety (WTS) voluntary crashworthiness standards has included development of several surrogate fixtures to facilitate the process and allow consistent evaluation of products (Figure 6). Commercial wheelchairs are tested for their suitability for use as motor vehicle seats using a surrogate, strap-type, four-point tiedown system that has been validated to have the nominal characteristics and dynamic response of commercial tiedown systems. In this case, wheelchair manufacturers can test with a single surrogate tiedown instead of the more costly process of testing their wheelchairs with each type of commercial strap-type tiedown. The surrogate tiedown was designed to create a more repeatable response than commercial tiedowns, which reduces variability in the test process and reduces the likelihood of failing and invalidating a test. Similarly, there is a surrogate wheelchair (SWC) representing a mid-sized wheelchair to test wheelchair securement systems and a surrogate wheelchair base (SWCB) to test third party wheelchair seating. Both of these fixtures were designed to provide a repeatable, durable response that offers a more cost-effective and efficient alternative to manufacturers having to test their products with a large number of commercial wheelchairs and frames. Testing with these surrogate fixtures is performed using the same midsize male ATDs used in assessing crashworthiness of vehicles.



Figure 6. Surrogate wheelchair tiedown (left), surrogate wheelchair (center), and surrogate wheelchair base (right).

These standards also include best practice recommendations for locating seatbelt anchorages to provide optimal belt fit. They also detail methods for ensuring that wheelchair components do not prevent placement of a vehicle lap belt across the occupant's pelvis.

### **Project Objective**

We hypothesize that wheelchairs meeting voluntary crashworthiness standards for use as seating in motor vehicles would meet current FAA standards for aircraft seats. During this three-year project, we will be testing this hypothesis. One task involves constructing test fixtures that will allow testing of wheelchairs to the FAA requirements for aircraft seats under the frontal impact condition, and testing different commercial wheelchairs that meet current WC19 requirements. A second task involves construction of a fixture that allows testing of wheelchairs to the vertical loading requirements of FAA aircraft seating, followed by testing different commercial wheelchairs to these requirements. The third task involves testing commercial wheelchairs to the static testing requirements using a fixture designed to accommodate wheelchairs. Should our

hypothesis be incorrect, we will develop and test solutions that might improve the performance of commercial wheelchairs relative to FAA seating requirements. With either hypothesis outcome, we will draft test procedures based on the initial tasks and work with a standards committee to include them as an annex to current crashworthiness standards to allow development of wheelchairs suitable for use as aircraft seating. We will also document results in reports that could be used to support requests to the FAA to move forward with allowing people to travel in their own wheelchairs on aircraft.

This interim report documents progress on initial tasks:

- Developing methods for performing static aircraft seating tests on wheelchairs
- Conducting static aircraft seating tests on five commercial wheelchairs
- Developing methods for conducting frontal dynamic aircraft seating tests on wheelchairs, including modeling to support methods development
- Conducting frontal aircraft seating tests on five commercial wheelchair models

## Adapting FAA Test Conditions for Wheelchairs

### Attachment Conditions

Best practice recommendations for securing wheelchairs is illustrated in Figure 7 [13]. The angle of the rear tiedown straps should be between 30 and 45 degrees with respect to horizontal and extend straight back from the securement brackets, parallel to the wheelchair centerline. The front straps should be anchored forward and spaced slightly wider than the wheelchair for increased stability. A front strap angle between 30 and 70 degrees with respect to horizontal is typical.

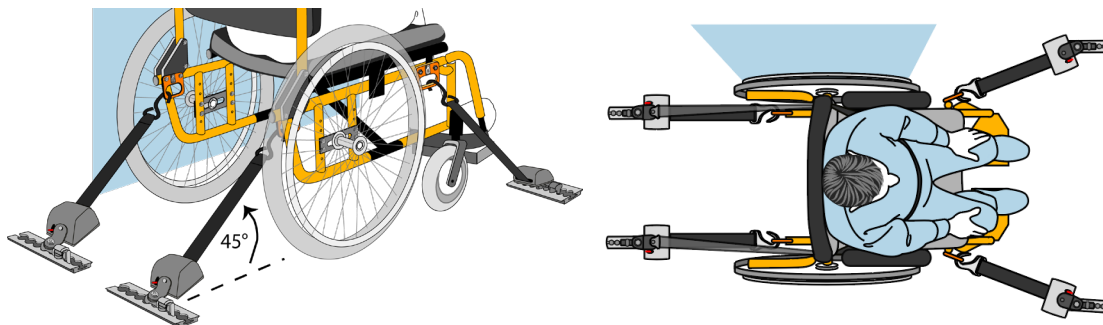


Figure 7. Illustration of best practice recommendations for securing wheelchairs with 4-point strap tiedowns.

These recommendations reflect the conditions used in WC18 and WC19 testing; securement points on wheelchairs are designed to perform best under these conditions. The specific language prescribed for securing wheelchairs with tiedowns in WC19 is extracted below, including adjustments and tension settings.

- 1) Vehicle anchor points should be symmetric about the longitudinal centerline of the wheelchair station. The wheelchair centerline should be aligned with the longitudinal centerline of the wheelchair station within +/- 3 degrees.

- 2) The fore-aft distance between front and rear anchor points should be  $1220 \pm 12$  mm ( $48 \pm 0.5$  in). An alternative fore-aft distance of  $1296 \pm 12$  mm ( $51$  in  $\pm 0.5$ ) is allowed to accommodate larger wheelchairs (or if trying to comply with ISO test procedures).
- 3) Laterally, the rear anchor points should be within  $\pm 25$  mm of the rear securement points on the wheelchair.
- 4) Laterally, the front anchor points should be aligned with or outboard relative to the front securement points on the wheelchair. Lateral distance should range from 300 to 760 mm (12 to 30 in).
- 5) Adjust the surrogate tiedown length to 495 mm (19.5 in). Attach the surrogate tiedowns to the four securement points on the wheelchair. With the rear tiedowns taut, measure the side-view angle of the rear tiedown straps between the anchor points on the floor and the hooks at the wheelchair.
  - a. If the angle is below 45 degrees, the strap adjustment is complete.
  - b. If this angle is above 45 degrees, lengthen the rear tiedown straps until the tiedown straps are within  $45 \pm 3$  degrees when secured to the rear anchor points.
- 6) When the desired length is achieved, tension the front tiedown using the ratchet mechanisms to a tension between 100 and 200 N (22 to 44 lbf).

Since a goal of this research program is to demonstrate that WC19 wheelchairs can meet the FAA testing requirements for aircraft seats, using the same tiedown geometry specified in WC19 with the FAA testing procedures would provide the most consistency and likelihood of success, as we would be loading the wheelchair securement points under the same conditions they are currently tested for compliance. Figure 8 shows a template used to check that the locations of the wheelchair securement points are in the allowable zone.



Figure 8. Fixture used to check that wheelchair securement points are in recommended zone.

To clarify the benefits of using this recommended geometry under FAA dynamic loading conditions, we conducted simulations comparing the response using this geometry to a more compact geometry where the floor anchors are directly below the wheelchair securement points. Figure 9 shows a comparison of kinematics under frontal loading between the recommended

tiedown geometry and a more compact vertical geometry, while Figure 10 shows the same thing under vertical loading. Under frontal loading, the wheelchair moves forward substantially more under vertical tiedowns compared to recommended tiedowns; wheelchair and ATD head excursions are also larger with the vertical tiedown geometry than the recommended geometry.

Figure 11 and Figure 12 compare the four tiedown loads between the recommended and vertical tiedown configurations. All of the vertical tiedown loads have higher peak values than those from the recommended geometry. In addition, the lap belt loads shown in Figure 13 are higher with the vertical geometry under both loading conditions.

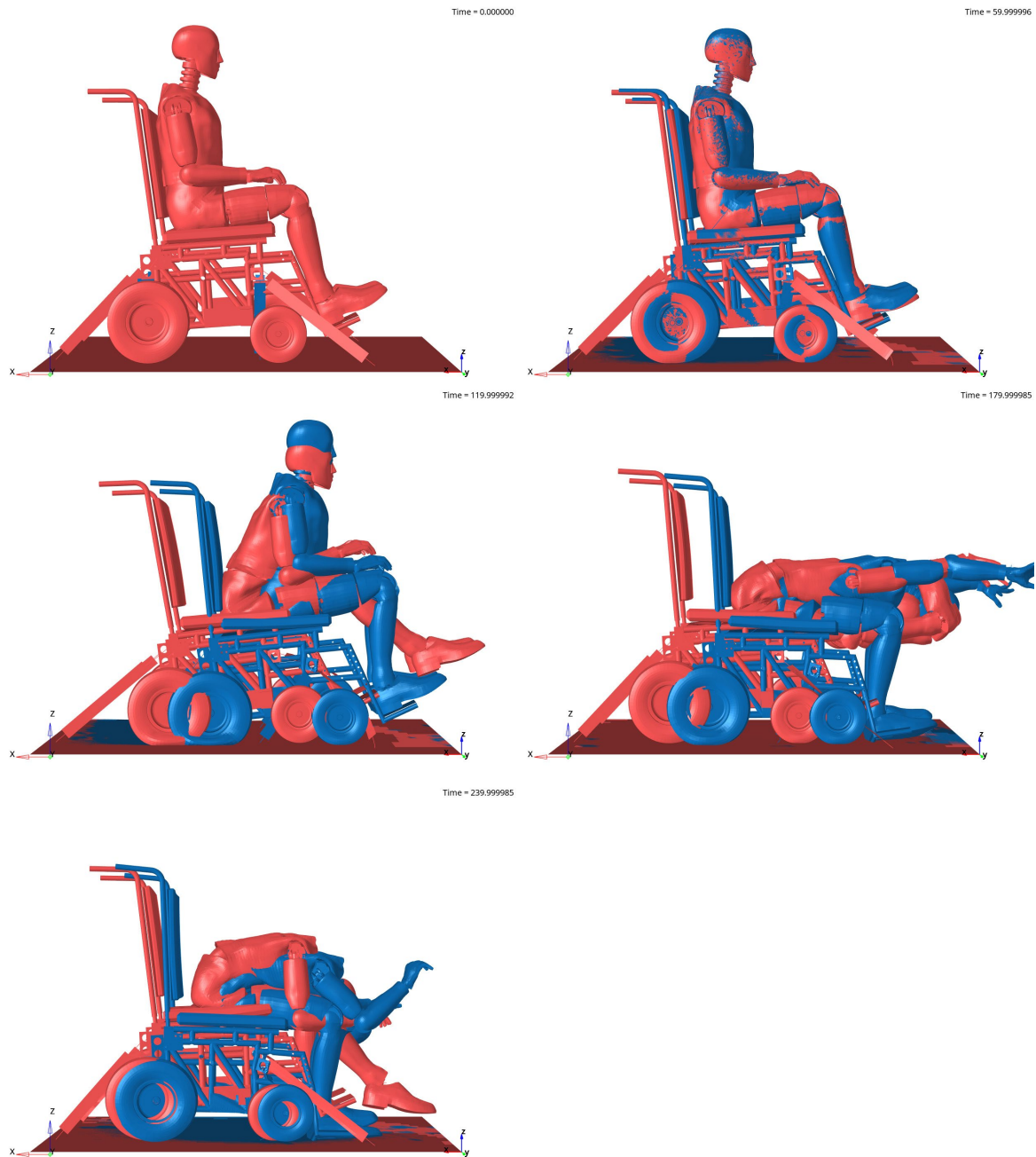


Figure 9. Comparison of kinematics under frontal loading conditions for recommended (red) and vertical (blue) tiedown geometry at 0, 60, 120, 180, and 240 ms.

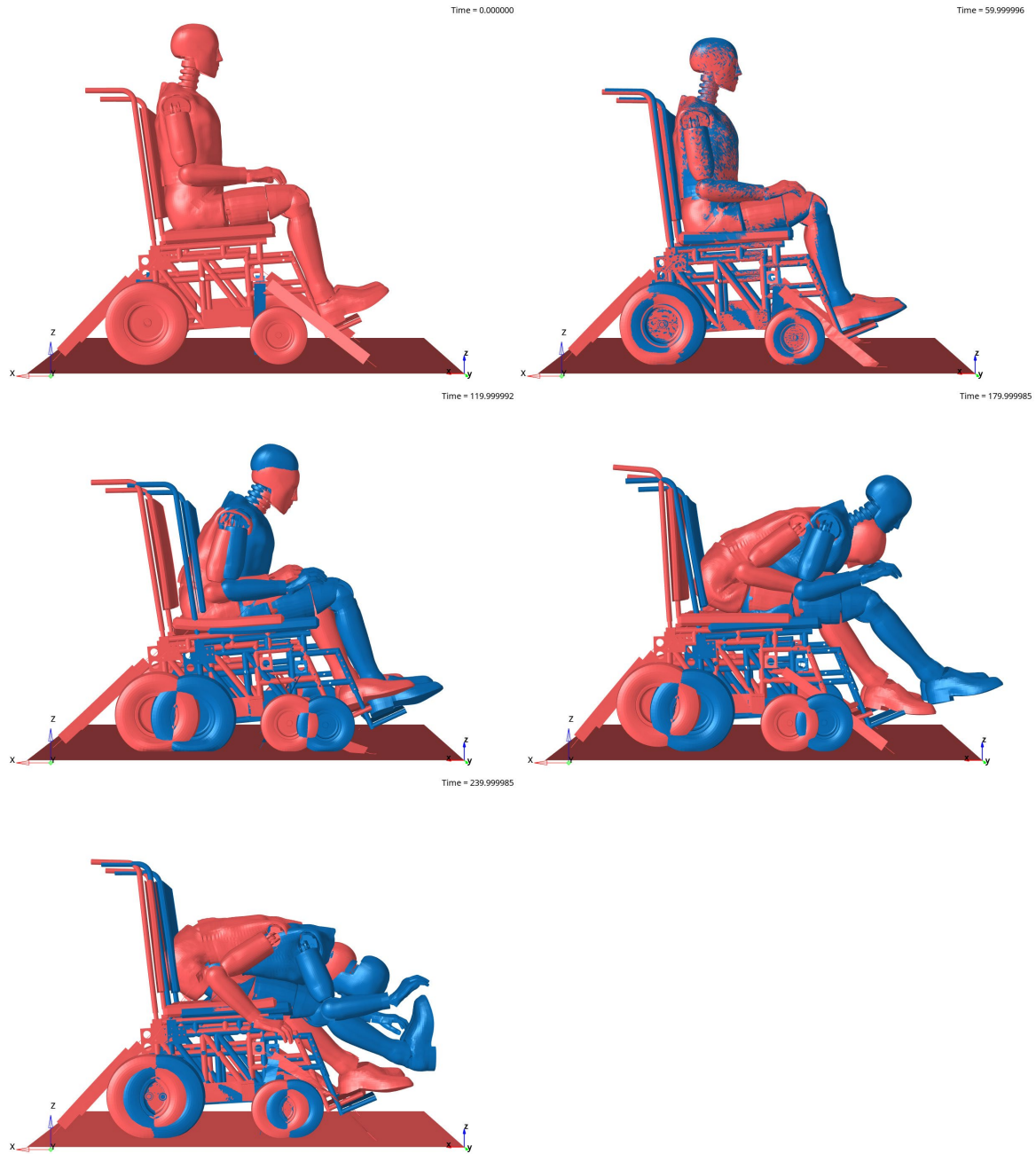


Figure 10. Comparison of kinematics under vertical loading conditions for recommended (red) and vertical (blue) tiedown geometry at 0, 60, 120, 180, and 240 ms.

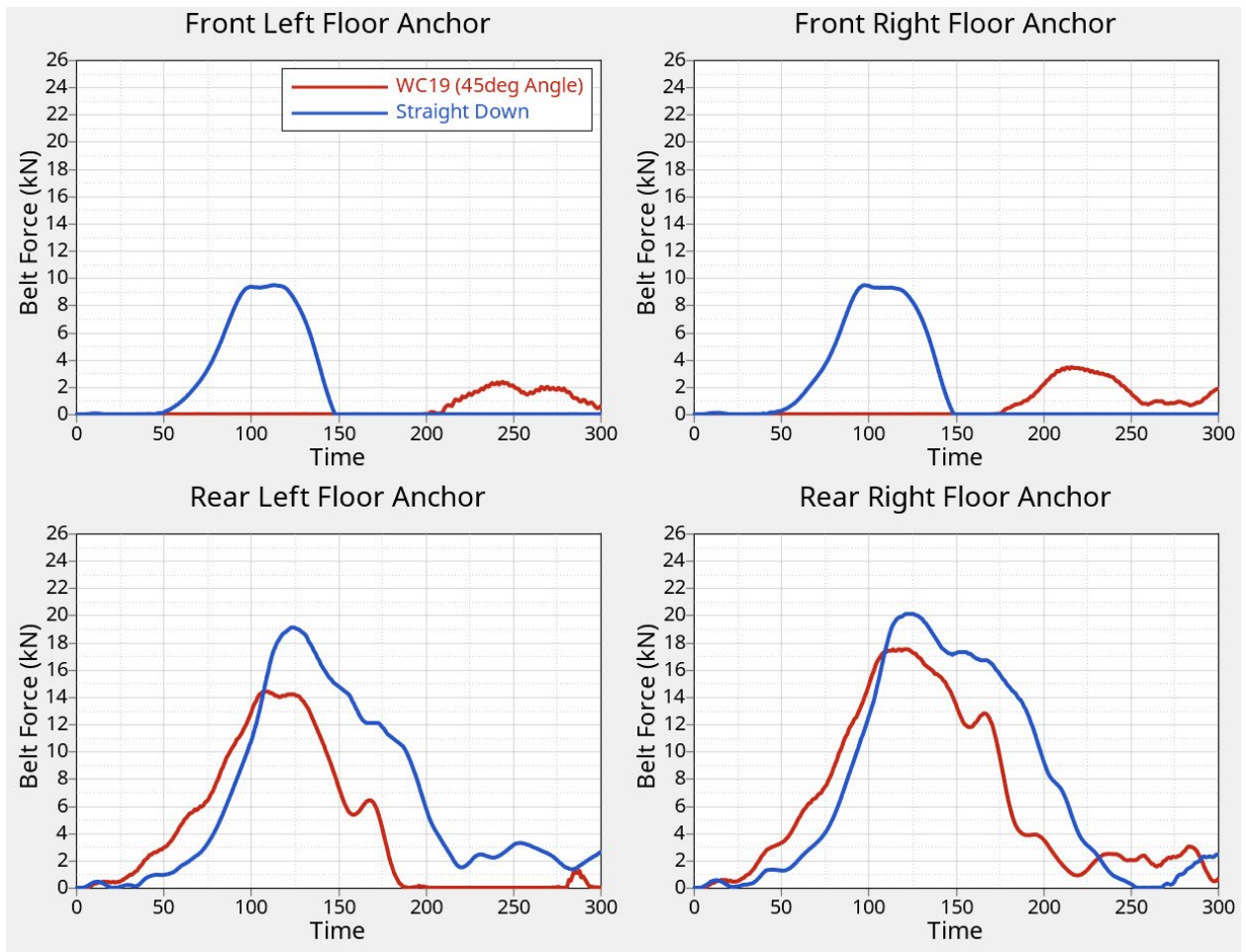


Figure 11. Comparison of tiedown loads under frontal loading for recommended (red) and vertical (blue) tiedown geometries.

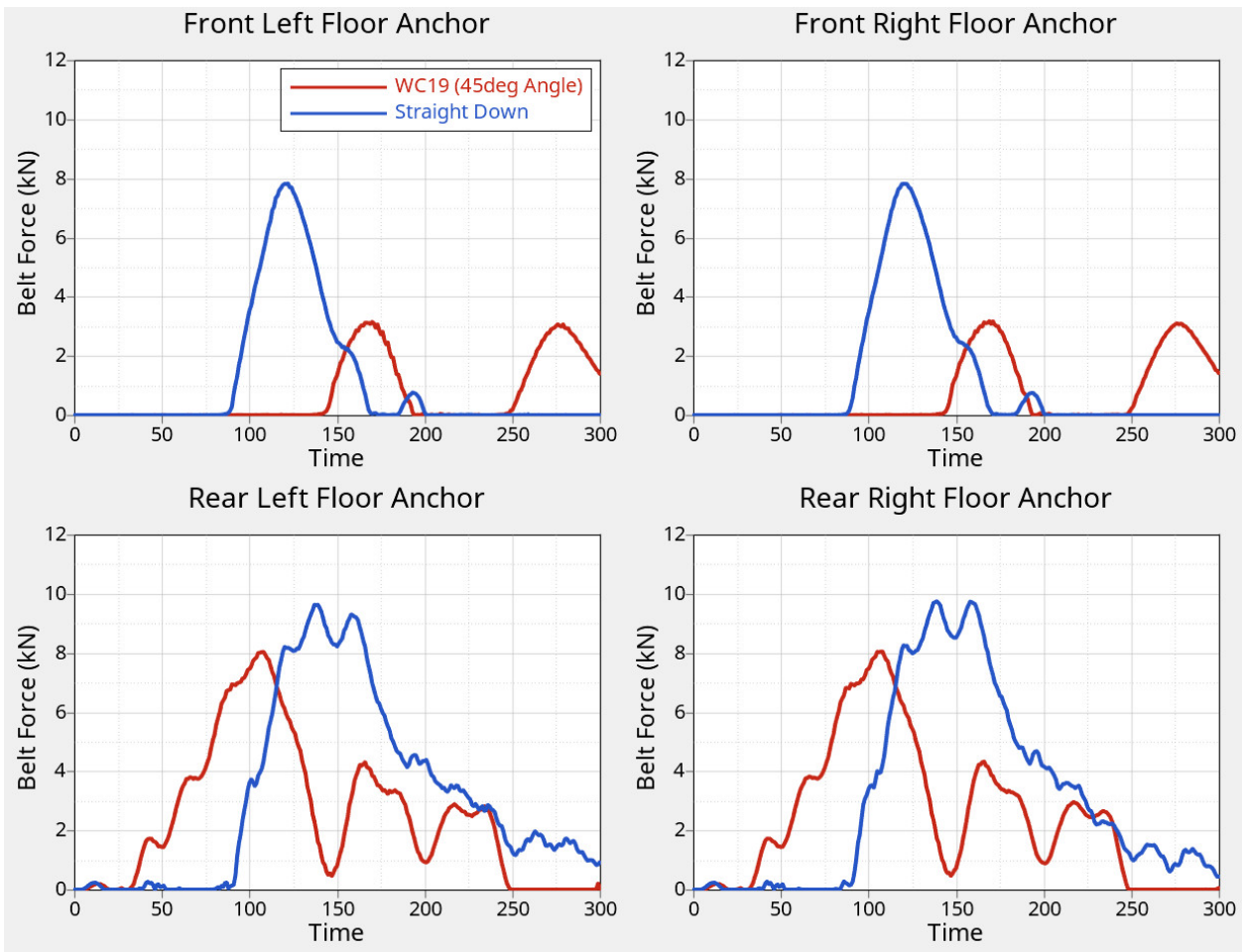


Figure 12. Comparison of tiedown loads under vertical loading for recommended (red) and vertical (blue) tiedown geometries.

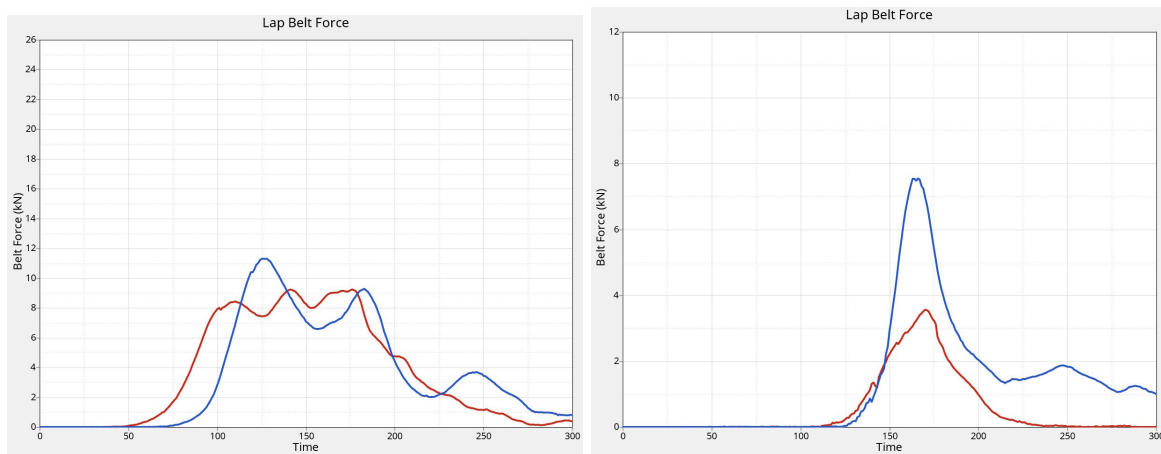


Figure 13. Comparison of lap belt loads for frontal (left) and vertical (right) for recommended (red) and vertical (blue) tiedown geometries.



WC19 uses surrogate 4-point strap tiedowns shown in Figure 14 to ensure consistent and repeatable performance of tiedowns when evaluating different wheelchairs. The Surrogate Wheelchair Tiedown and Occupant Restraint System (SWTORS) was used to secure all wheelchairs tested in both static and dynamic testing conditions.



Figure 14. Rear (left) and front (right) SWTORS used to secure wheelchairs during WC19 testing.

#### **Wheelchair Station Location Potential Contact with Bulkhead**

The minimum space required for a wheelchair station in ground vehicles is 760 mm (30 in) wide and 1220 mm (48 in) long to accommodate the majority of wheelchair sizes [32]. In buildings, the recommended size for alcoves is 864 mm (34 in) and 1524 mm (60 in) long [33]. The locations for tiedowns are supposed to be outside of this clear space, but this is not always the case on vehicle installations.

Advisory Circular 25.562-1B [11] specifies that seats that could be located adjacent to a bulkhead should be tested with a simulated bulkhead if the space between the SRP of the seat and the bulkhead is less than 102 cm (42 in). These conditions require measurement of femur load and calculation of HIC should head contact occur.

We conducted a geometric analysis to determine whether a bulkhead representation should be included in our frontal dynamic test fixture, as well as where to locate the wheelchair within the wheelchair station. We used available data from commercial wheelchairs previously tested at UMTRI using WC19 test procedures, with examples of pretest photos of a manual wheelchair and power wheelchair are shown in Figure 15. Since vehicle manufacturers use the H-point, an approximation of the hip joint center, as a reference in motor vehicle design, a previous effort digitized landmarks on sideview pretest photos of 75 different wheelchairs. Landmarks include the most rearward points above and below the seatpan, the most forward point, the center and contact for each set of wheels (2 or 3 pairs), the H-point, the seat bight (junction of the seat cushion and seatback), and locations of the rear and front securement brackets. The lines superimposed on the photos show the main structural components of the seat, the location of the tiedown securement points, and the center points and ground contact points of each wheel. These

data were aligned so the rear tiedown anchor is at the origin. The orange points in Figure 15 represent the bight of each wheelchair.

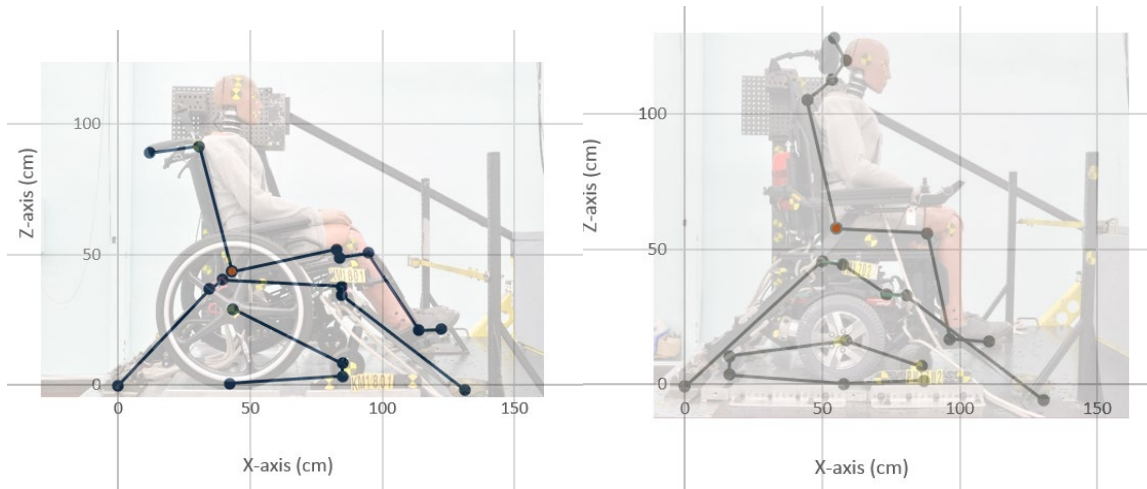


Figure 15. Key landmarks on a manual wheelchair (left) and power wheelchair (right).

Based on the methods in SAE AS6909 for determining the SRP of an aircraft seat, the bight of an occupied wheelchair is a reasonable representation of the SRP for a wheelchair. Figure 16 shows a plot of the variation in bight location when the origin is set to the rearmost point on the wheelchair rather than the rear tiedown location. For the 75 wheelchairs we digitized, the x-value of the bight ranges from 9 to 55 cm and the mean value is 29 cm. The manual wheelchair in Figure 15 has a bight near the average value, while the power wheelchair has the maximum forward value.

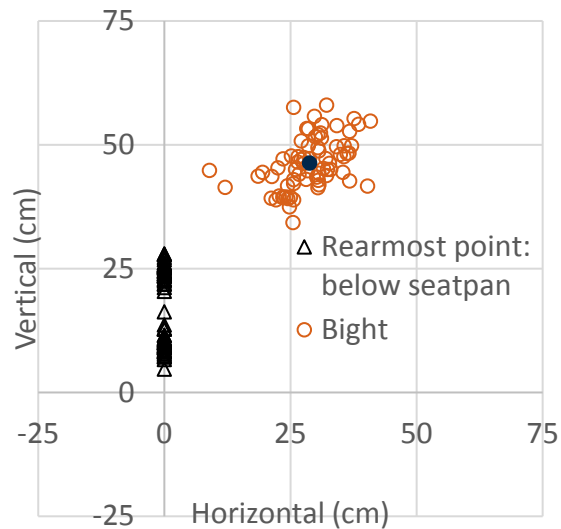


Figure 16. Variation in bight location of 75 wheelchairs, when rearmost point of wheelchair is the origin.

Figure 17 and Figure 18 show two options for placing wheelchair stations within a wheelchair station. In Figure 17, we show a 152 cm (60 in) long wheelchair station (maroon line), representing the recommended length of alcoves in buildings, which is similar to the situation of navigating into an aircraft row from a narrow aisle. The tiedowns are located at the rear edge of the station ( $x=0$ ) and the wheelchair securement geometry reflects recommended practice. The yellow line placed 107cm (42 in) from the bulkhead shows that the average SRP is behind the estimated contact range, although the most forward SRP is approximately 10 cm (4 in) forward of this location. Because the available space for a wheelchair station on an aircraft would be the same regardless of the wheelchair size, this configuration likely reflects a realistic testing environment for future aircraft wheelchair stations. Figure 18 shows an alternative setup that is more consistent with aircraft seat test procedures, where the SRP is placed 107 cm (42 in) from the bulkhead. The plot indicates that some longer wheelchairs may not fit within the station, and it may not be feasible to achieve recommended WC19 tiedown geometry. Based on discussion with our FAA advisors, we did not include a bulkhead representation in our testing to reflect the more likely condition of fixed rear tiedown anchor location shown in Figure 17, with more than half of wheelchairs having low potential for head contact based on geometry.

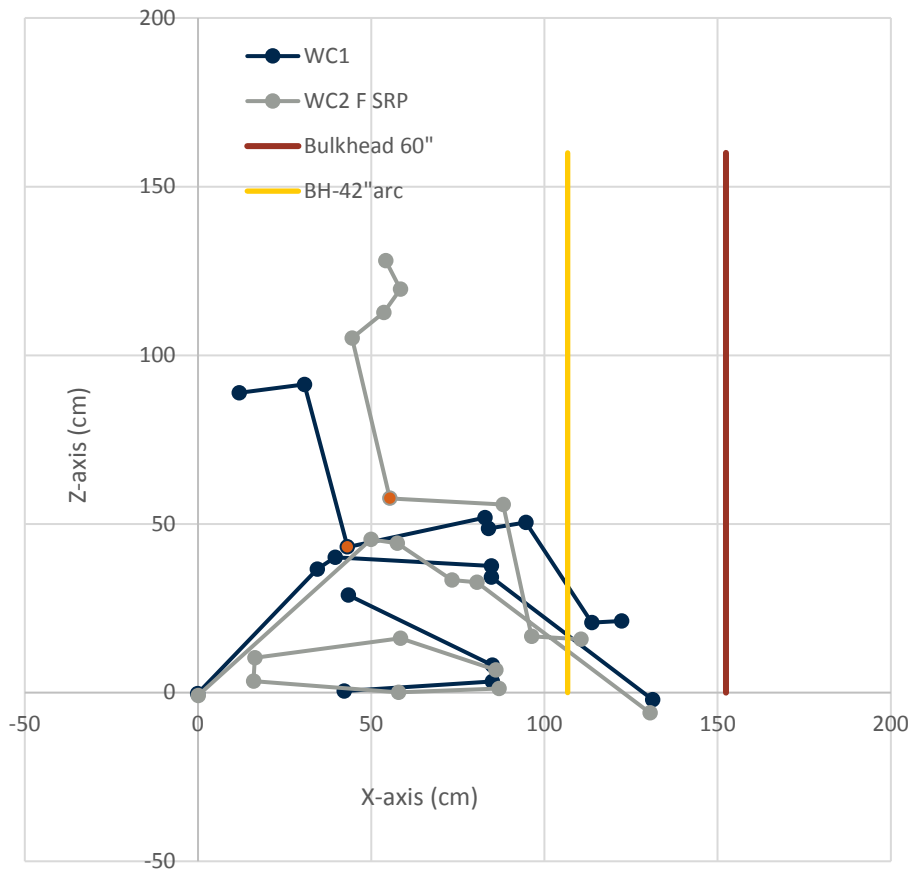


Figure 17. Suggested geometry with tiedowns located at rear of station, bulkhead located 152 cm (60 in) forward, indicating that the average SRP would be rearward of the 107 cm (42 in) arc requiring representation of bulkhead during testing.

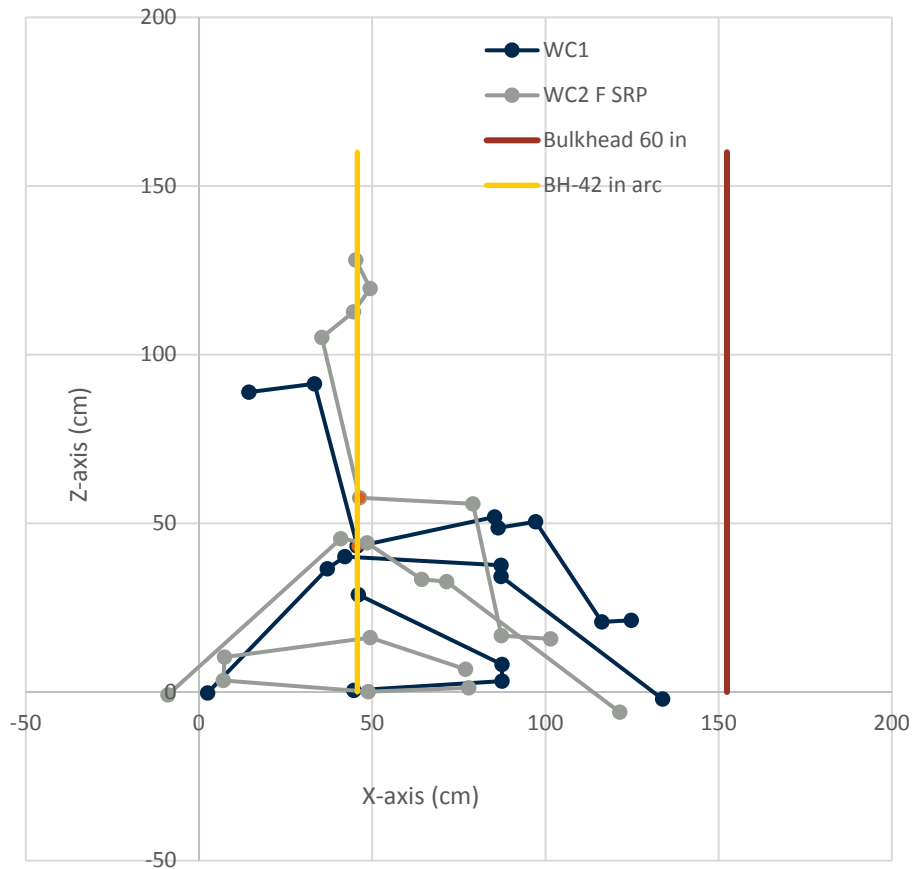


Figure 18. Alternative geometry with SRP located 107 cm (42 in) from bulkhead, showing there may be insufficient space to secure longer wheelchairs appropriately.

### ATD Selection

The original ATD used for testing aircraft seats is the Hybrid II midsized male (Part 572:B). When the Hybrid III ATD was introduced as a more realistic ATD for assessing occupant safety in motor vehicles, it was not accepted as equivalent to the Hybrid II for evaluating aircraft seats [34]. The main reason was a difference in response during the vertical testing condition, where a requirement is that the ATD must have a compressive axial force less than 1500 lb. Differences in the pelvis design may also contribute.

A project was undertaken to make a kit for the Hybrid III ATD that made it respond more closely to the Hybrid II in areas most important for aircraft seat assessment. Changes involved:

1. Using an 1891 Hybrid II Lumbar Load Cell and pelvic adaptor block.
2. Using a Hybrid II lumbar column.
3. Using a different upper-lumbar-thorax adaptor.
4. Using a Hybrid II abdominal insert.
5. Using Hybrid II upper leg elements.
6. Using a Hybrid II chest flesh, with a notch cut in the chest flesh.

While we used the recommended FAA Hybrid III ATD for our frontal testing, we note the differences here, as our simulations to investigate how different factors might affect testing choices used the standard Hybrid III model we have available.

### Sled Pulse

14 CFR Part 25 specifies that the frontal dynamic test pulse have a minimum delta V of 48 kph and a peak acceleration of 16 g achieved within 90 ms, but no minimum rise time is specified. The Federal regulation does not prescribe the shape, but AS8049 describes the ideal shape as triangular.

Figure 19 compares the ideal FAA frontal pulse with a trapezoidal pulse produced by the UMTRI sled that meets the specifications but not the ideal shape. The sharper rise time of the UMTRI pulse likely produces more severe loading than required. We performed simulations with the surrogate wheelchair base (SWCB) and a standard Hybrid III midsize male ATD to evaluate the potential effect of the different pulse shapes.

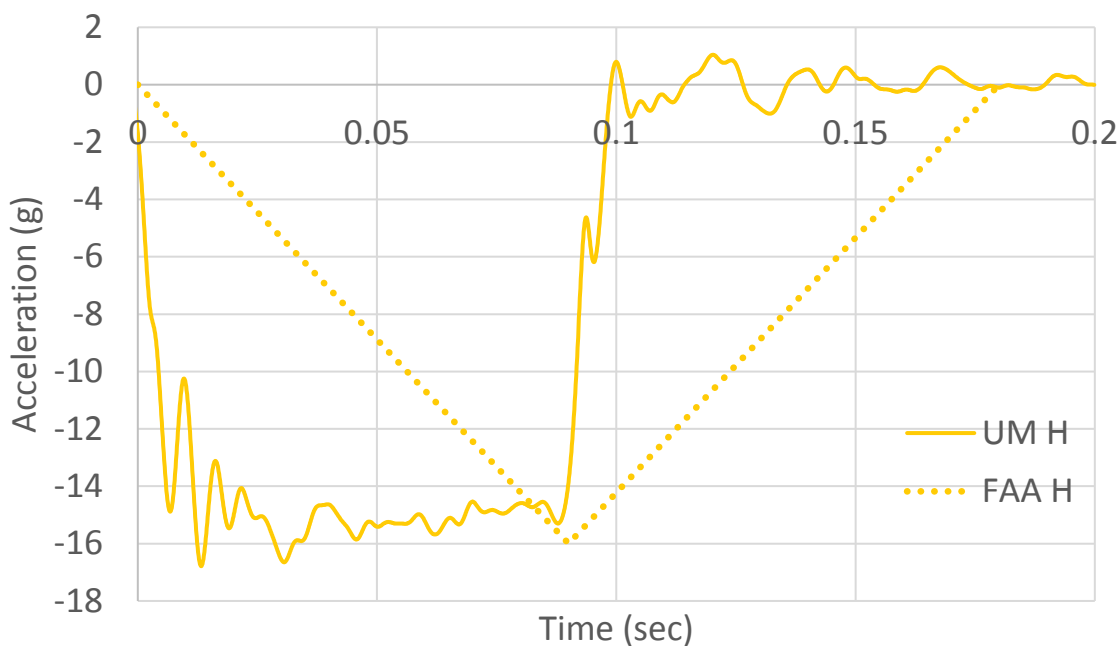


Figure 19. Comparison of ideal and UMTRI versions of the FAA horizontal pulse.

A comparison of the kinematic differences arising from the pulse characteristics is shown in Figure 20. The UMTRI pulse is the red ATD while the triangular pulse is blue. The UMTRI pulse causes the ATD to begin moving sooner, but the position at peak is similar for both conditions. Plots of the head and pelvis x and z excursions shown in Figure 21 confirm this observation. Both pulses produce maximum x displacements near 825 and maximum z displacements around -810 mm, but the peaks occur about 40 ms later with the triangular pulse. The pelvis x excursion is slightly higher with the UMTRI pulse, and the difference in peak timings is also about 50 ms. However, the pulses produce nearly identical trajectories for both

the head and pelvis shown on the right column of Figure 21. This result matches those from an earlier FAA evaluation of triangular vs. trapezoidal pulses [35].

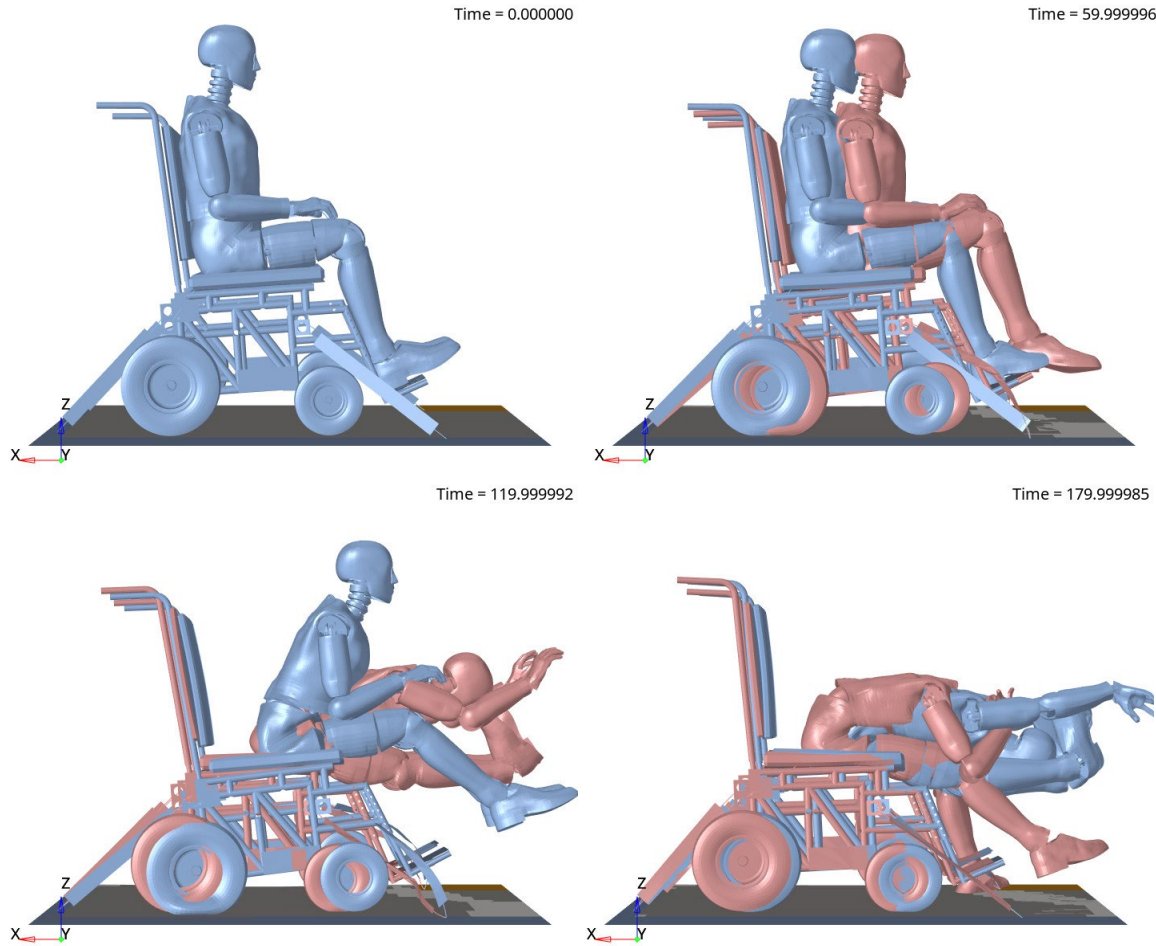


Figure 20. Comparison of kinematics between the UMTRI and triangular versions of the FAA pulse.

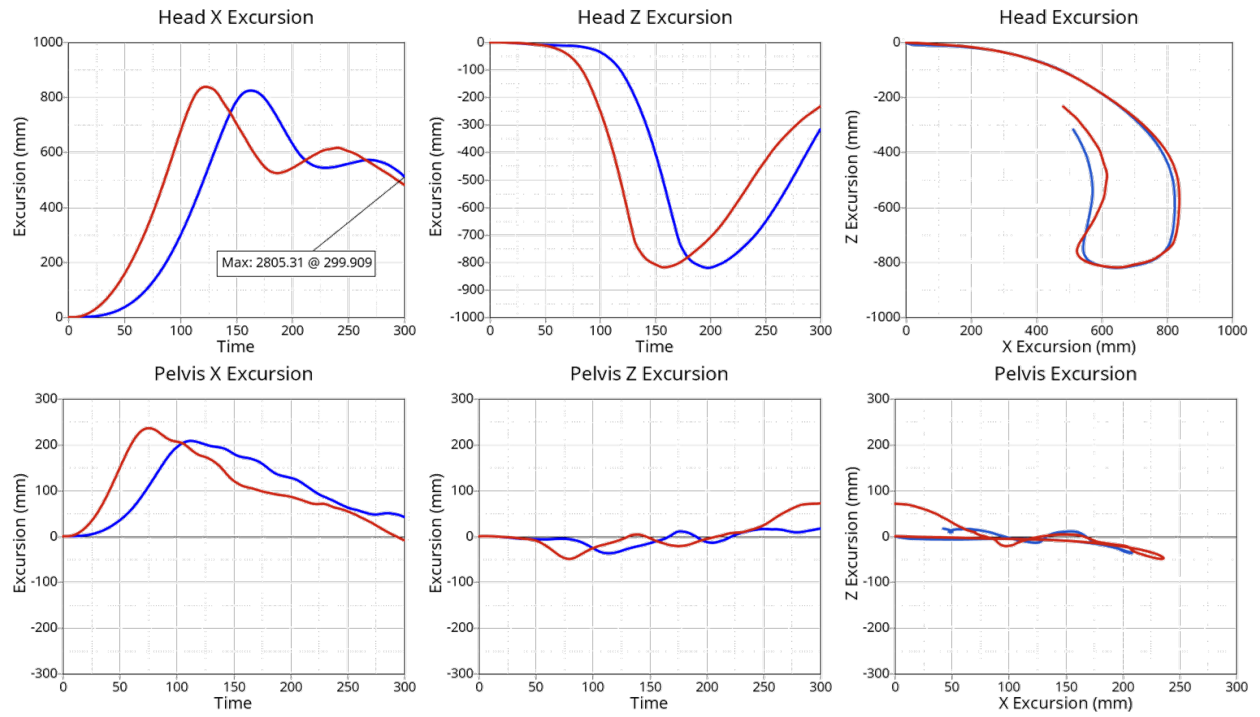


Figure 21. Comparison of head and pelvis excursions for UMTRI pulse (red) and triangular pulse (blue).

Differences in simulated ATD signals are shown in Figure 22 and Figure 23. Results include resultant head, chest, and pelvis acceleration, ATD-to-seat force, WC-to-floor force, seatbelt-to-ATD contact force, and lumbar axial force. For each comparison, the peak values occur about 40 to 50 ms earlier with the UMTRI pulse and are slightly higher (excluding spikes in head acceleration resulting from head to leg contact).

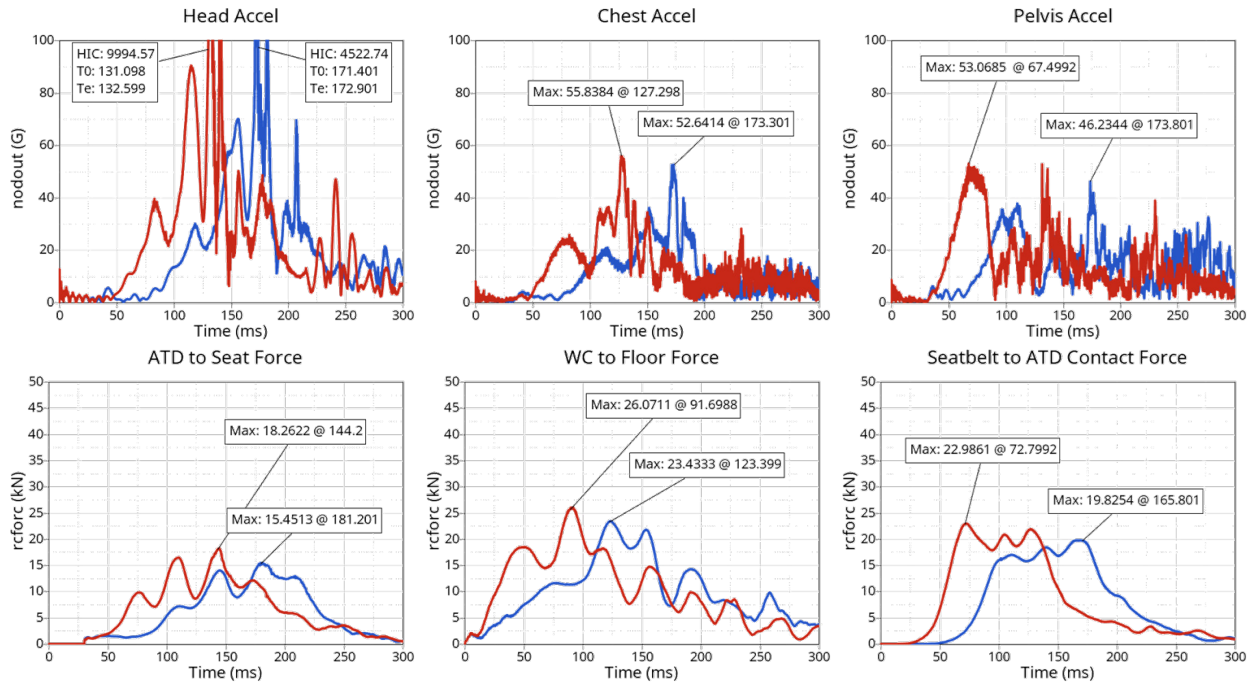


Figure 22. Comparison of resultant head, chest and pelvis accelerations (top row) and ATD-to-seat force, WC-to-floor-force, and seatbelt-to-ATD contact force between UMTRI (red) and triangular (blue) frontal FAA pulse conditions.

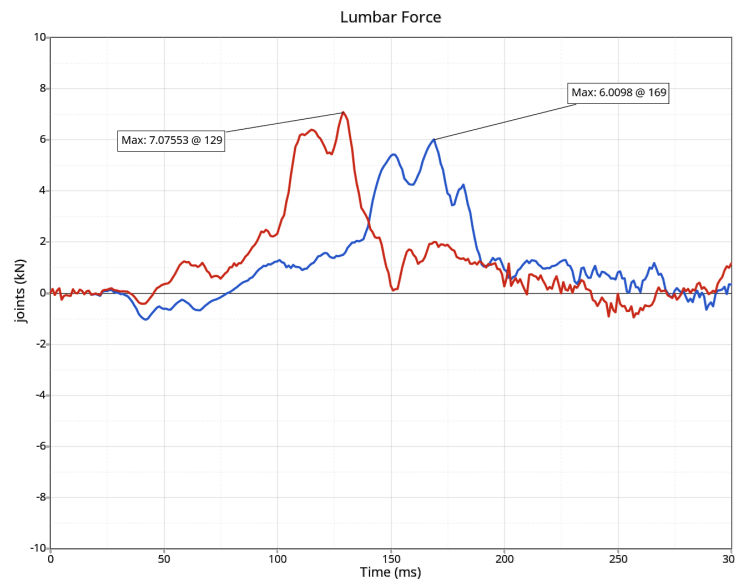


Figure 23. Comparison of peak lumbar force between UMTRI and triangular frontal FAA pulse conditions.



These simulations show that peak excursions match in magnitude but not timing. The UMTRI pulse provides loading conditions that meet or exceed ideal pulse loading, so wheelchairs that pass requirements using our pulse should also meet requirements using a more triangular pulse.

### **Yaw, Pitch, and Roll**

With WC19 testing, the wheelchair faces forward and is aligned with the direction of sled travel. For FAA frontal dynamic testing, a key difference is that the wheelchair is yawed 10 degrees to the left or right relative to the primary forward direction of vehicle movement. The current wheelchair testing set up was rotated 10 degrees to adapt to this condition.

The FAA procedure also calls for simulating the effects of a deforming floor on an aircraft seat structure through deformable anchor points that simulate  $\pm 10$  deg pitch and  $\pm 10$  deg roll. Since wheelchairs would be secured by flexible 4-point strap tiedowns rather than rigid hardware used to secure aircraft seats, we hypothesized and the FAA agreed that simulating the deformable floor elements would be less relevant because the tensions in the tiedowns would change but the tiedowns would not fail.

Figure 24 shows a comparison of the kinematic differences at 0, 60, 120, and 180 ms, where the fixed floor condition is in gold and the deforming floor condition is in purple. Figure 25 compares forces and excursions. The peak values of ATD-to-seat force and WC-to-floor force are slightly higher with the deformed floor condition, while the peak head X excursion and pelvis X excursion are slightly higher with the fixed floor condition. Based on the minimal differences and consultation with our FAA advisors, for our first dynamic assessments of wheelchairs under frontal FAA conditions, we did not simulate the deformed floor condition.

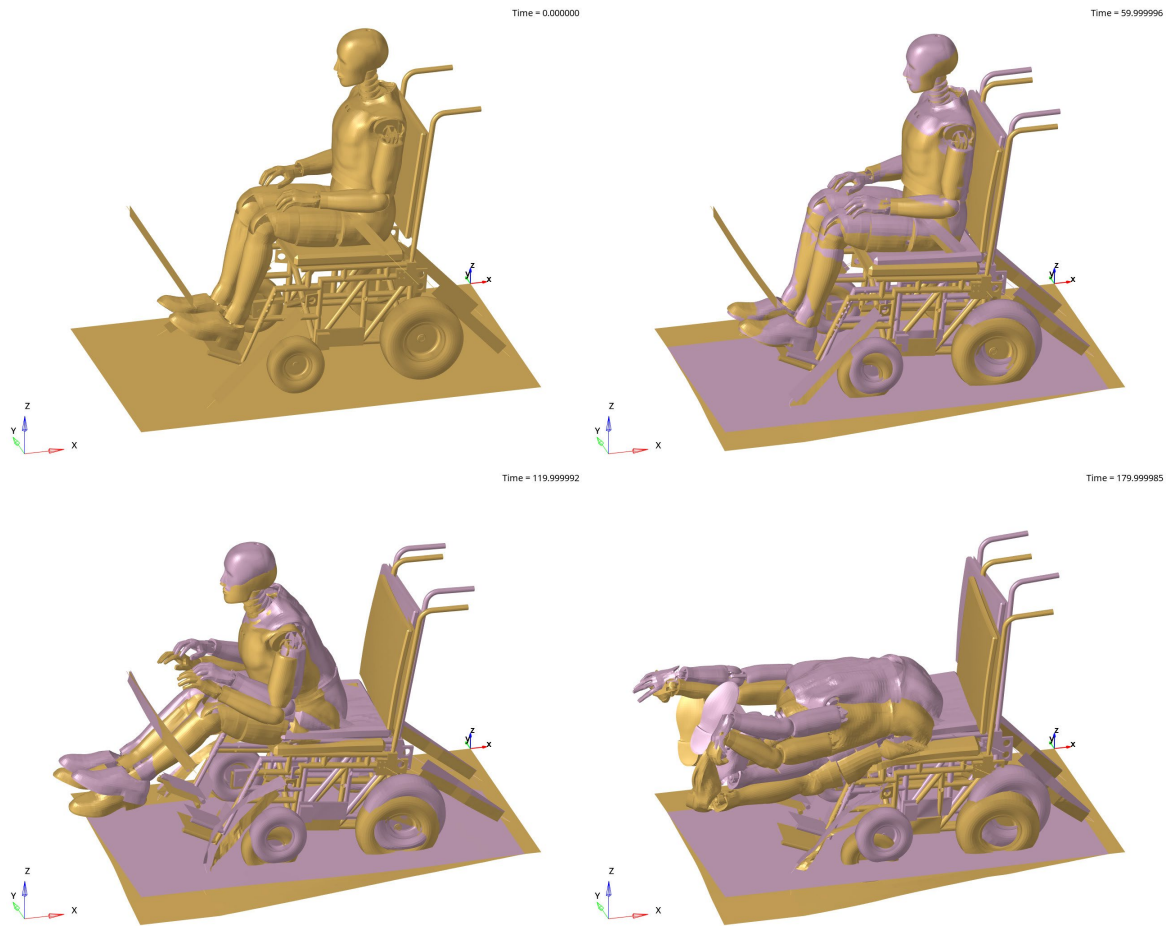


Figure 24. Simulations showing the effect on ATD and wheelchair kinematics with and without prescribed floor deformation (gold=fixed, purple=deformed).

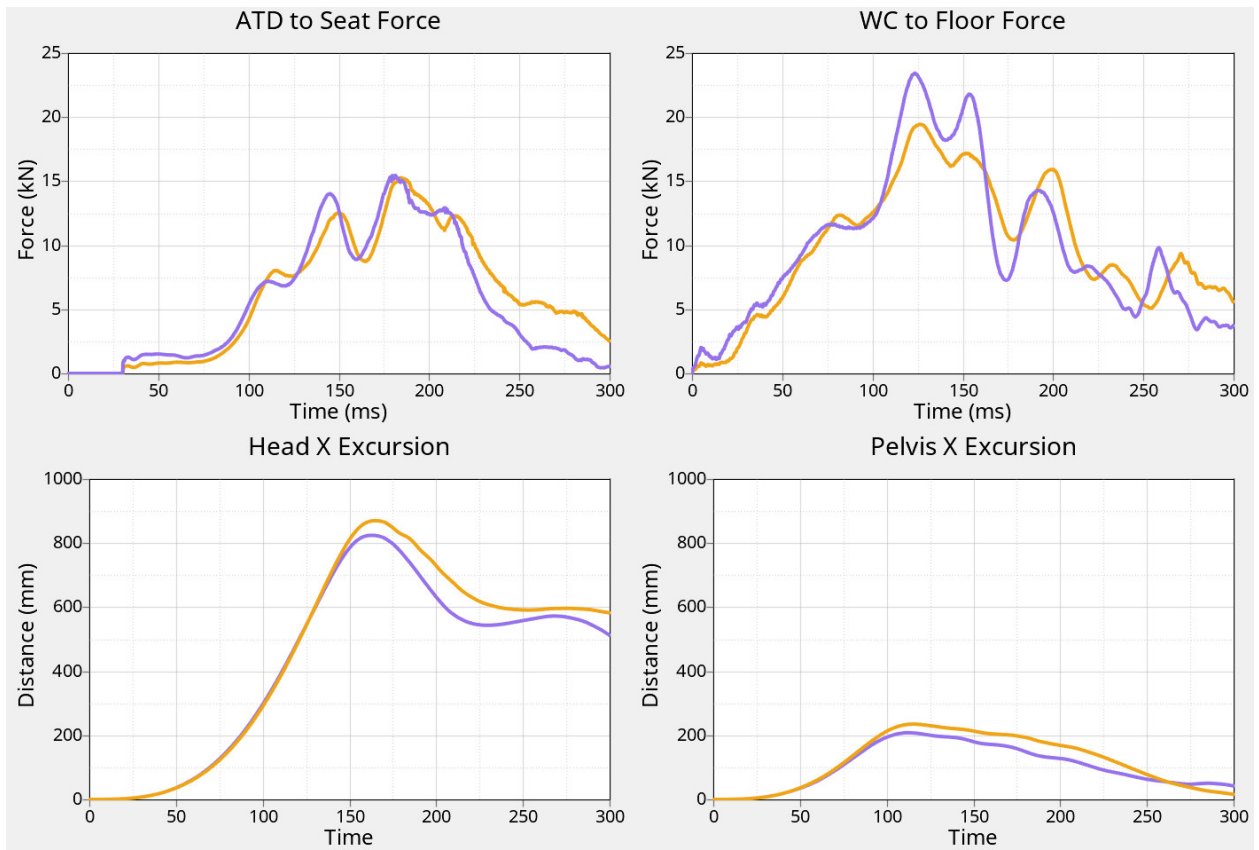


Figure 25. Simulations showing small differences in ATD-to-seat force, WC-to-floor force, peak head X excursion, and pelvis X excursion with and without prescribed floor deformation (gold=fixed, purple=deformed).

## Wheelchair selection

To maximize use of the wheelchairs used in testing, we planned to test wheelchairs first in static testing, followed by either frontal or vertical testing. The first six commercial wheelchairs listed in Table 1 were selected to span a range of characteristics. All wheelchairs tested were selected from our list of products meeting WC19 requirements and came with a wheelchair-anchored crashworthy lap belt, as required by the standard, with one exception. The Jazzy with Captain Seat no longer meets WC19 compliance. While it has dedicated securement points, they are now marked as not being suitable for occupied securement, although we used them during testing. While WC19 test procedures also include options for testing with a vehicle-mounted shoulder belt, we did not test with an additional shoulder belt because most aircraft seats use only a lap belt. For consistency with other passengers, an additional anchor point for attaching a shoulder belt is unlikely to be provided on aircraft.

Table 1. Summary of first set of wheelchairs purchased for testing.

<b>Wheelchair Model</b>	<b>Abbrev.</b>	<b>WC Mass (lb)</b>	<b>WC Mass (kg)</b>	<b>Type</b>
<b>Surrogate Wheelchair Base</b>	SWCB	125	57	Surrogate fixture
<b>KiMobility Catalyst 5</b>	KMC5	23	10	Manual, folds laterally
<b>TiLite ZRA</b>	TLZ	30	14	Manual, rigid
<b>Convoid Safari SFT 810</b>	CVS	45	20	Manual, folds laterally and fore-aft
<b>Sunrise QM 710</b>	SQ710	380	173	Power base with complex seating
<b>Quantum Q6 Edge 2</b>	QE2	356	162	Power base with suspension
<b>Jazzy with Captain Seat</b>	JCS	198	90	Power base with pedestal seating

## Static testing

### Methods

For static testing, we adapted the test procedures found in SAE Aerospace Standard AS8049, revised in November 2020. We used the procedures associated with seat type A-T (transport airplane) specified in 14 CFR Part 25. We focused on static tests and did not consider flammability requirements.

For this task, we hypothesize that wheelchairs meeting RESNA WC19 frontal crashworthiness standards should be able to meet FAA 25.561 static tests requirements for aircraft seats when secured by a 4-point strap tiedown system. As mentioned in the current relevant standards section, the static tests involve loading in upward, forward, lateral, downward, and rearward directions, with the required force level varying for each direction.

The standard specifies use of a body block to transmit load to the seat. We purchased a fixture meeting the specifications. The fixture contains a loading hook positioned 270 mm above the base and 215 mm forward of the back such that load applied through the hook meets the requirements for where to apply the load. Prior to testing with commercial products, we evaluated each condition with the SWCB. This fixture was used rather than the SWC, because the width of the body block would not fit between the fixed armrests on the SWC.

Figure 26 through Figure 28 shows examples of the test setup for frontal, rear, and lateral static test conditions. We conducted tests on our wheelchair test buck, to allow use of the standard tiedown configurations. For this task, we purchased a winch with a capacity of 27kN (6000 lb), which is higher than the maximum required for the most extreme loading condition of a 185 kg wheelchair in a frontal test. We constructed a mounting bracket for the winch that was anchored to the front of the sled buck, which allows adjustability of the winch so it can be aligned vertically with the loading hook with wheelchairs of different seat heights.

For the up and down pull tests, we were able to move the sled to a location with a lower ceiling and horizontal cross beam. As shown in Figure 29, we mounted the same winch on the cross beam to apply vertical load through the body block. For the downward condition, we mounted pulleys to provide downward loading via the overhead winch. For the downward condition, we did not use the body block, instead building a fixture that distributed the load over the seat.



Figure 26. Example setup for frontal static pull test of QE2.

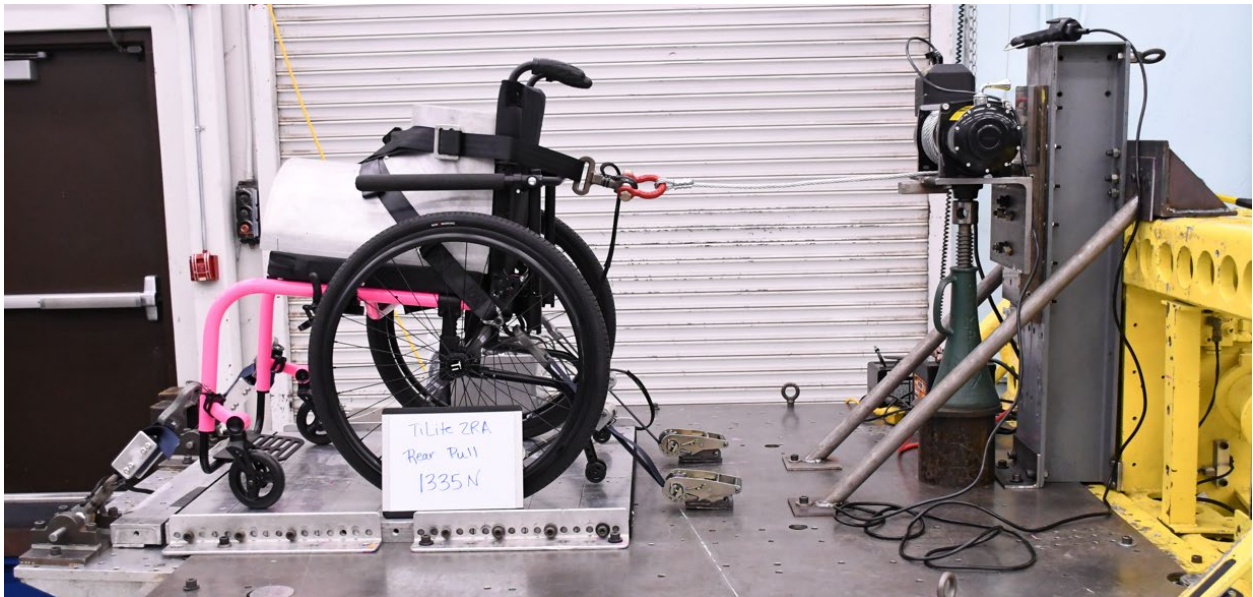


Figure 27. Example setup for rear static pull test of TLZ.



Figure 28. Example setup for lateral static pull test of JCS.

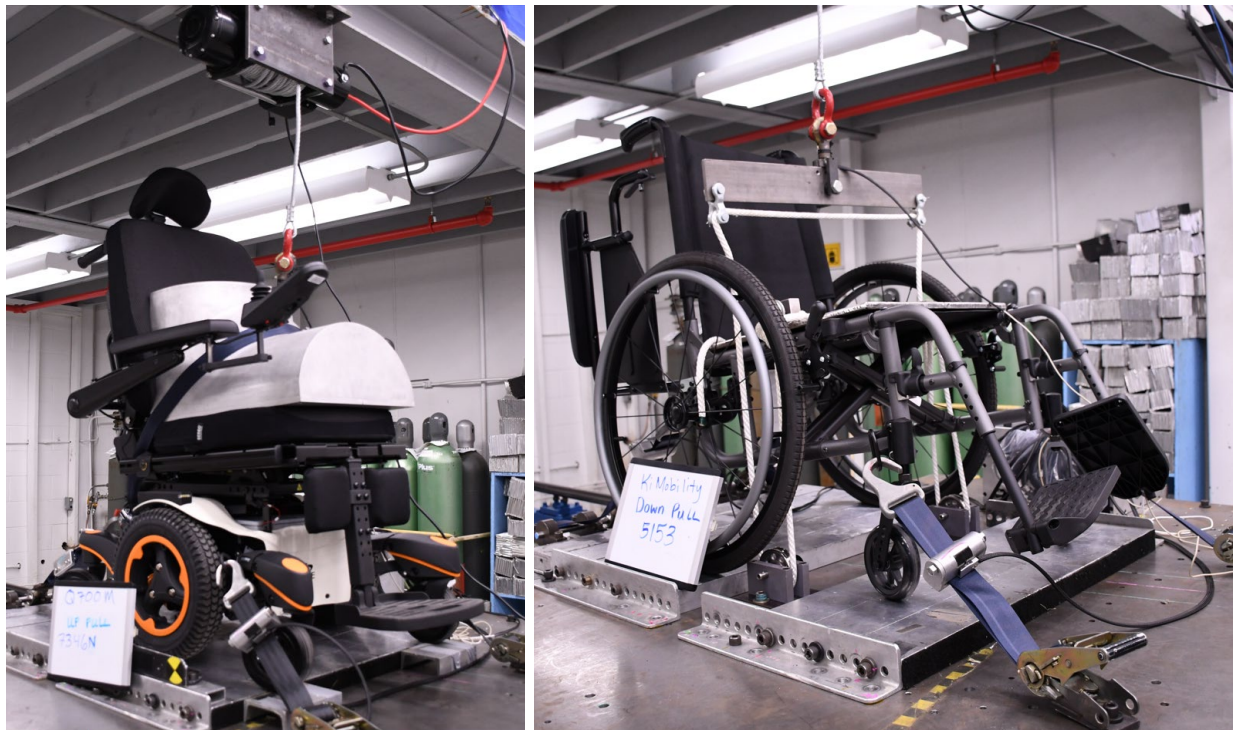


Figure 29. Examples of upward pull test of SQ700 (left) using winch mounted to ceiling beam, and downward pull test of KMC5 (right) using sam overhead winch and pulleys to apply downward load.

In all tests, the body block was restrained using the crash-tested lap belt attached to each wheelchair. The wheelchair was secured to the test platform using the SWTORS specified in WC19. Pictures of the test setup were taken before and after each test. A camera was used to record each test. A load cell was used to record the force applied through the winch, which was displayed in real time near the test location. The winch was operated manually, with the technician turning on the winch until the target load was reached, then held for three seconds before using a hammer to quickly disengage the winch.

Table 2 lists the total mass of each wheelchair and the target applied load for each direction. The range of applied loads is 1335 N for the TLZ rear to 22039 N for the SQ710 frontal test. Static testing of the CVS was postponed until frontal testing was completed.

Table 2. Wheelchair masses and target applied load for each static test direction.

Wheelchair Model	Mass units	WC Mass	Total Mass (+77.1 kg)	Force Units	Frontal (*9 g)	Lateral (* 4 g)	Downward (*6 g)	Upward (*3 g)	Rear (*1.5 g)
<b>SWCB</b>	lb	125	295	lbf	2657	1181	1771	886	443
	kg	57	134	N	11818	5252	7878	3939	1970
<b>Ki Mobility Catalyst 5</b>	lb	23	193	lbf	1738	772	1158	579	290
	kg	10	88	N	7729	3435	5153	2576	1288
<b>TiLite ZRA</b>	lb	30	200	lbf	1801	800	1200	600	300
	kg	14	91	N	8010	3560	5340	2670	1335
<b>Sunrise QM 710</b>	lb	380	550	lbf	4955	2202	3303	1652	826
	kg	173	250	N	22039	9795	14693	7346	3673
<b>Quantum Q6 Edge 2</b>	lb	356	526	lbf	4739	2106	3159	1580	790
	kg	162	239	N	21077	9368	14051	7026	3513
<b>Jazzy with Captain Seat*</b>	lb	198	275	lbf	3315	1473	2210	1105	552
	kg	90	167	N	14744	6553	9829	4915	2457



Our initial plan to document deformation is illustrated in Figure 30. We have a portable Sense 3D scanner that we have been using to capture the geometry of wheelchairs for modeling efforts on other tasks. We were able to scan wheelchairs post-test and planned to use MeshScape software to calculate the amount of residual deformation from the static tests. Unfortunately, it was challenging to line up each scan to achieve an adequate measure of deformation.

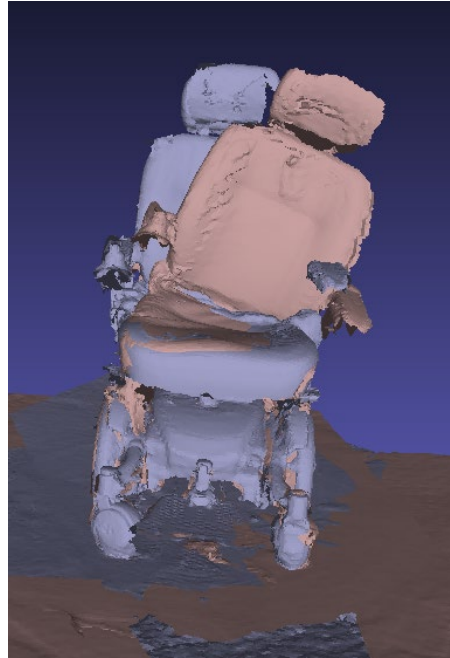


Figure 30. Illustration of deformation using pre- and post-test 3D scans of wheelchairs.

For future tests, we plan to document deformation two ways. First, we will use the Sense scanner to record the 3D shape, but we will do it before and after each static test with the wheelchair secured with the tiedowns to allow better alignment of pre- and post-test scans. Second, we will mark key landmarks on the wheelchair with targets and use a FARO arm 3D coordinate measurement device to record their location before and after each test.

## Results

Results presented in this section include photos of the wheelchairs at the time of maximum static loading before release, photos of damaged wheelchair components, and plots of static loads for each wheelchair.

Photos of rear static testing are shown in Figure 31. We were able to achieve the target load level and duration in all tests, and none of the wheelchairs showed visible damage post test. The downward static photos are in Figure 32. Again, none of the wheelchairs showed visible damage post test. Figure 33 shows photos of each wheelchair during the upper static loading tests. Figure 34 shows damage to the JCS, which was the only wheelchair that did not pass this condition. In this test, the seat lifted off the post that connects it to the base.

Figure 35 shows the peak lateral static testing photos. The upper left picture of the SWCB shows the loading fixture shifting off the seat, which might be expected among other products that do not have armrests. The two manual wheelchairs did not sustain damage, except the KMC5 left tire popped; this would be allowed under WC19 testing. The three power wheelchairs sustained damage as shown in Figure 36 through Figure 38. Lateral testing of the QE2 (Figure 36) resulted in left armrest deformation and overall permanent lateral shift. The damage to the JCS shown in Figure 37 was a permanent deformation of the seat relative to the base. For the damage to the SQ710 shown in Figure 38, the seat tipped permanently relative to the base, the left armrest post deformed relative to the seat, and the right front tiedown deformed around the tire, prohibiting easy motion of that wheel.

Frontal test photos are shown in Figure 39. The two manual wheelchairs passed the frontal tests but all three power wheelchairs were damaged. The QE2 damage shown in Figure 40 involved breaking of the mechanism that allows changing the seat position, such that the seat was permanently rotated about 40 degrees forward post test. For the SQ710 shown in Figure 41, the seat completely came off the base. For the JCS shown in Figure 42, the plywood seat fractured and the top crossbar on the base for holding the seat was substantially deformed.

While we were unable to confidently quantify the amount of residual deformation using scans as planned, the damage to all three power wheelchairs was substantial enough to conclude that they would not meet the allowable deformation limits.



Figure 31. Photos of peak rear static loading for SWCB (upper left), TLZ (upper right), KMC5 (middle left), JCS (middle right), QE2 (lower left), and SQ710 (lower right.)

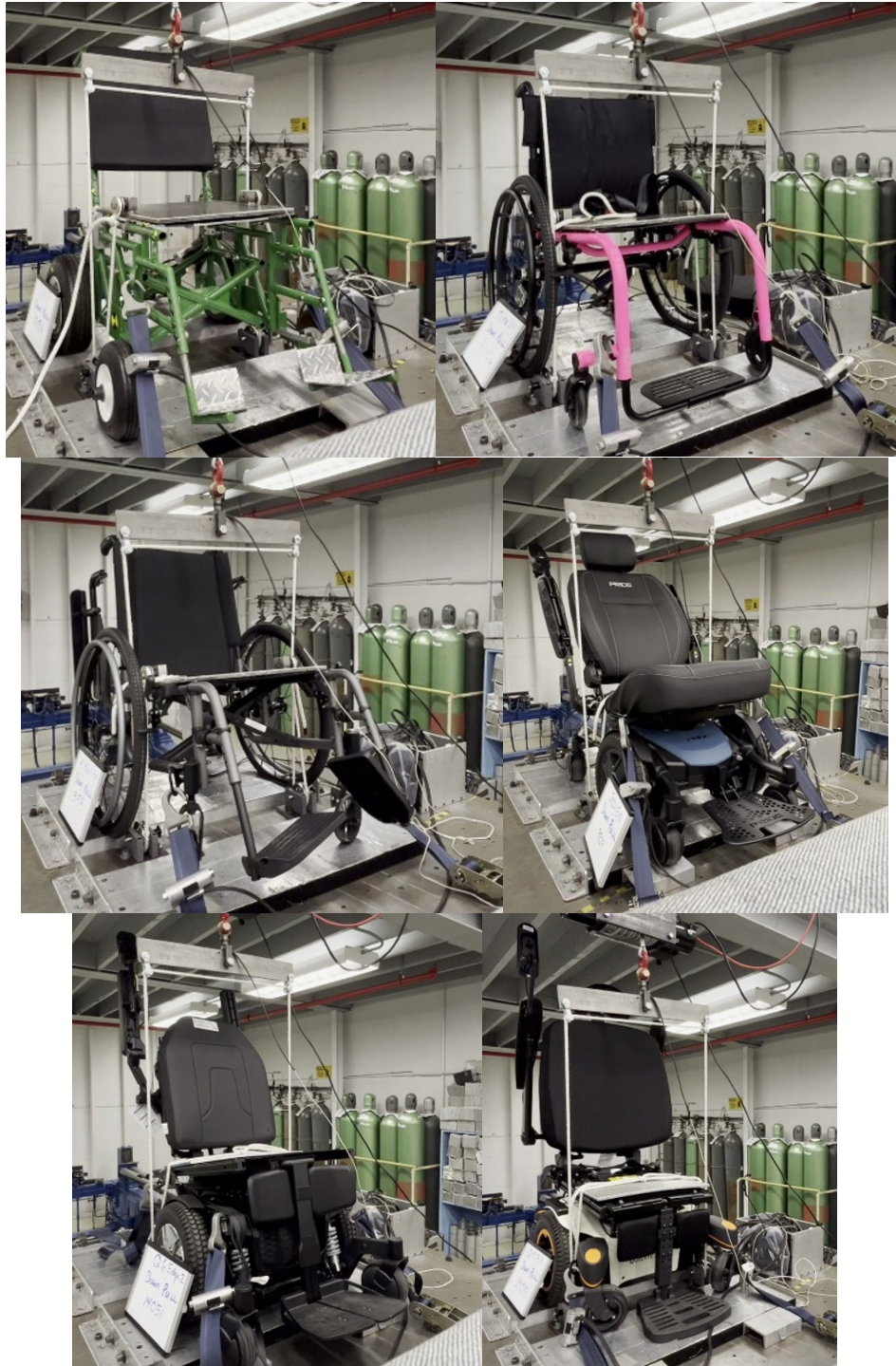


Figure 32. Photos of peak downward static loading for SWCB (upper left), TLZ (upper right), KMC5 (middle left), JCS (middle right), QE2 (lower left), and SQ710 (lower right.)



Figure 33. Photos of peak upward static loading for SWCB (upper left), TLZ (upper right), KMC5 (middle left), JCS (middle right), QE2 (lower left), and SQ710 (lower right.)



Figure 34. Closeup photo of JCS seat detached from base after upward loading test.



Figure 35. Photos of peak lateral static loading for SWCB (upper left), TLZ (upper right), KMC5 (middle left), JCS (middle right), QE2 (lower left), and SQ710 (lower right.)



Figure 36. Damage to QE2 sustained during lateral static testing.



Figure 37. Damage to JCS sustained during lateral static testing.



Figure 38. Damage to SQ710 sustained during lateral static testing.



Figure 39. Photos of peak frontal static loading for SWCB (upper left), TLZ (upper right), KMC5 (middle left), JCS (middle right), QE2 (lower left), and SQ710 (lower right.)



Figure 40. Damage to QE2 sustained during lateral static testing.



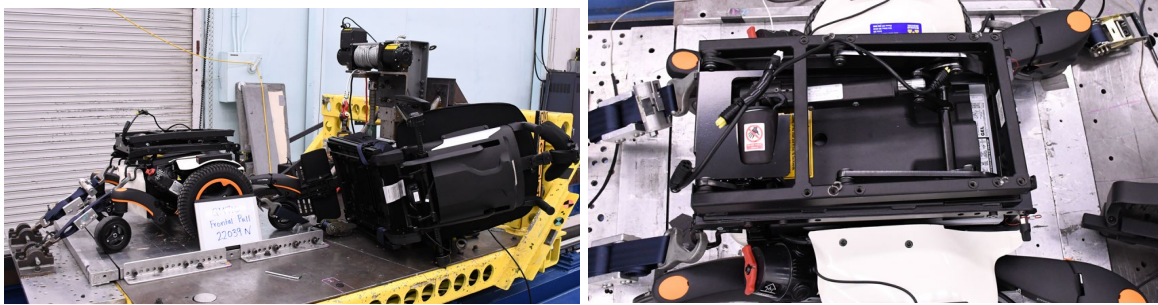


Figure 41. Damage to SQ710 sustained during lateral static testing.



Figure 42. Damage to JCS sustained during lateral static testing.

Figure 43 through Figure 47 show plots of the static loads recorded in tests for each wheelchair. On all these plots, solid lines show data while dashed lines indicate the target static load to be held for 3 sec. Time zero is set to be the time at which the target load is achieved, or 3 sec before failure if not achieved. For the TLZ shown in Figure 43, it passed requirements in all directions. While the lateral load fell slightly below target after 1.5 sec, we expect that it would pass the requirements. The KMC5 (Figure 44) also met all requirements. The left rear tire deflated during the lateral pull but this is not a failure per WC19.

For the QE2 (Figure 45), it passed the rear and downward static tests. For the upward test, there was no permanent damage, but we could not achieve the target force for the entire duration, because the seat frame started pulling up due to scissor action tilt mechanism. For the lateral tests, it was damaged and we ran out of winch stroke before the target load was achieved. For the frontal static test, we could not achieve target load before seat frame broke off of base at the rear.

For the SQ710 (Figure 46), it passed the rear and down static tests. For the upward pull, there was no visible damage but the target load was not maintained for the entire 3 second window. During the lateral test, the chair deformed extensively and the winch bottomed out before the target load was achieved. For the frontal static test, the seat frame broke completely off the base before the target static load was achieved.

For the JCS (Figure 47), it only passed the downward and rear tests. However, the back support started to recline during the rear test. During the upward pull, the seat frame pedestal pole pulled

out of base and separated before max load was obtained. During lateral loading, the seat plywood cracked and the seat started to pull of the base before maximum loading was achieved. Under frontal loading, the maximum load was not achieved.

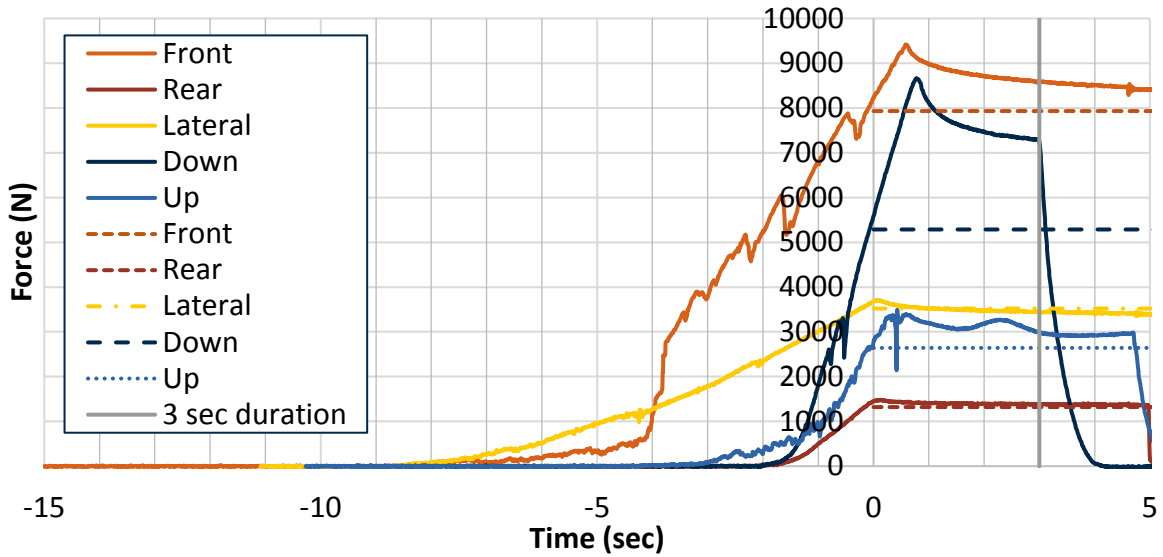


Figure 43. Static test results for TLZ.

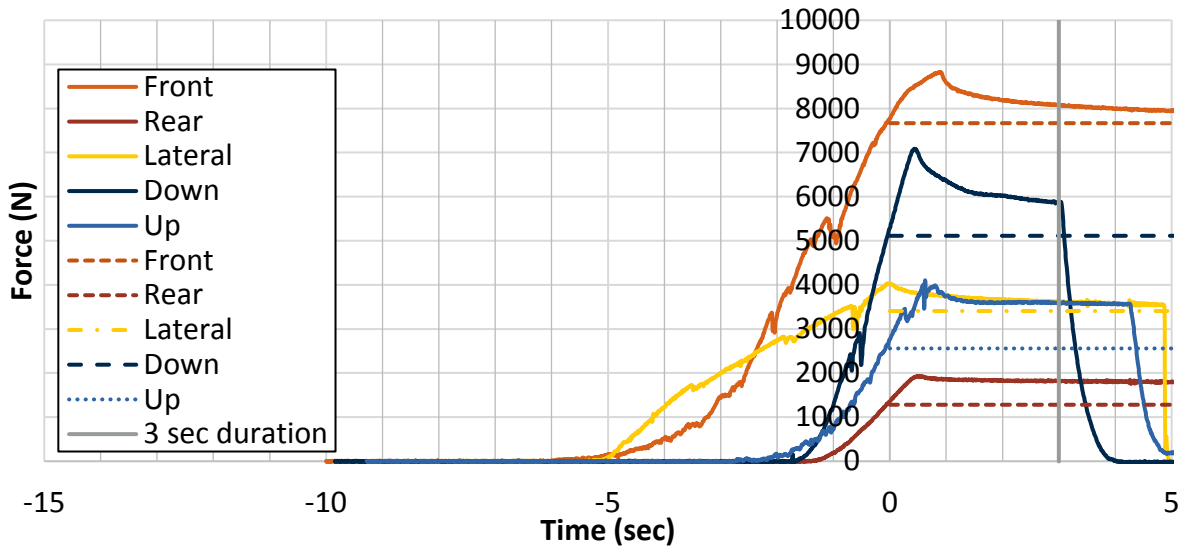


Figure 44. Static test results for KMC5.

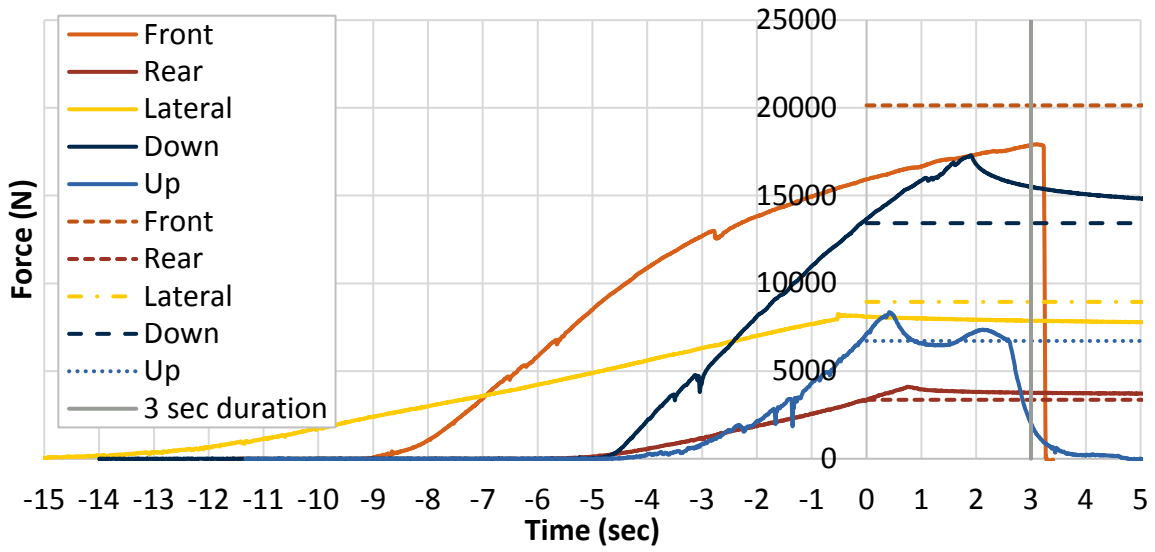


Figure 45. Static test results for QE2.

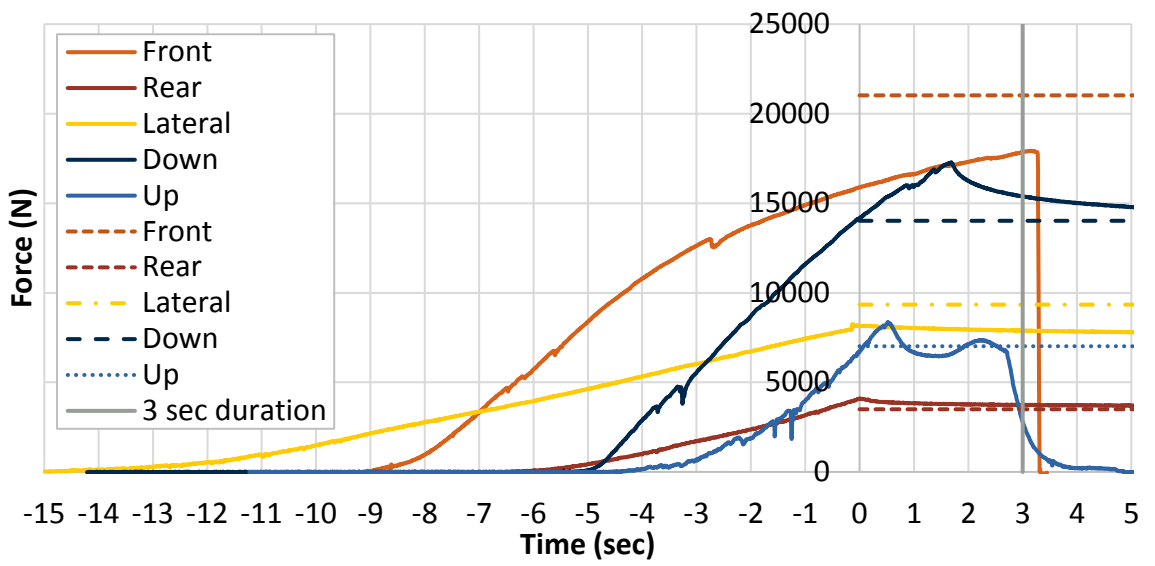


Figure 46. Static test results for SQ710.

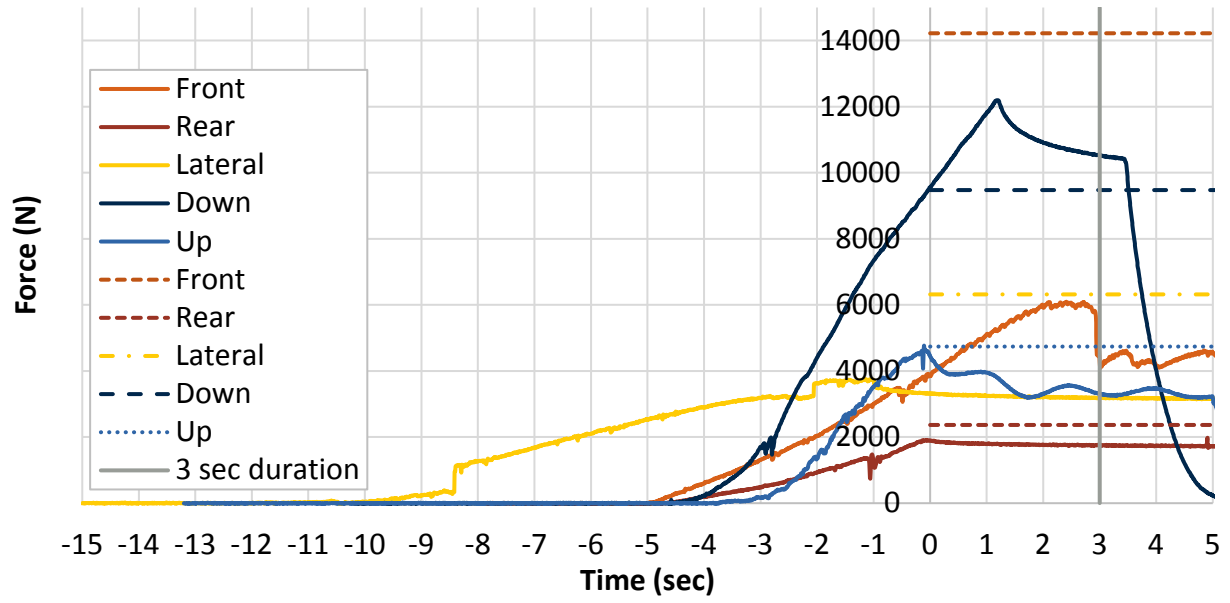


Figure 47. Static test results for JCS.

## **Dynamic Frontal Testing**

### **Methods**

For the dynamic testing, the FAA loaned UMTRI one of their FAA-Hybrid III ATDs. It was instrumented with triaxial accelerometers in the head, chest, and pelvis, as well as load cells in the upper and lower neck and lumbar spine. Additional measured signals were tiedown and belt loads. All signal data were gathered and filtered using SAE J211 protocols.

Video data were used to record five views that include overhead, left side (perpendicular to sled), right side (perpendicular to sled), right side (perpendicular to wheelchair), and right rear (to capture rebound kinematics). The video data were used to assess overall kinematic response of the wheelchair and ATD, including the head trajectory. Post-test observations and measurements recorded the physical damage and deformation of the wheelchair. Any detached hardware was noted and described.

The wheelchair was placed and secured using the procedures in RESNA WC19, with the exception that the wheelchair was rotated 10 degrees clockwise from the forward direction of sled travel. The ATD was also placed in the wheelchair using the methods prescribed by WC19; no modifications to the seating procedure were required with the FAA version of the H3 ATD. The leg strap allowed by WC19 to prevent unrealistic lower extremity kinematics was not used during testing. A FARO arm 3-D coordinate measurement system was used to record pretest location of ATD and wheelchair.

Appendix B contains a draft test procedure for evaluating wheelchairs under frontal aircraft seating conditions. The tasks are modified versions of WC19 procedures, revised to accommodate FAA seating procedure requirements.

Table 3 summarizes the dynamic frontal test matrix. Because of damage to some wheelchairs during static testing, some alternatives were used that had been previously tested, so column three lists the type of prior testing. We also note the prior testing type because we had concerns that the manual wheelchairs that passed the static testing without visible damage may have been weakened and affect the ability to pass the frontal dynamic test; we delayed static testing of the CVS for this reason. Column four lists the abbreviations used for each test on subsequent plots to indicate the type of wheelchair and previous testing. The SWCB was tested first to both confirm procedures and to demonstrate how similar it is to production wheelchairs under FAA testing conditions.

The last column of Table 3 shows the type of occupant restraint. In all tests but WA2307, the wheelchair-anchored (WA) lap belt (required as an option by WC19) was used to secure the ATD. Test WA2307 used a wheelchair previously tested to ISO 7176-19, where a wheelchair-anchored lap belt is not required. For tests WA2304 through WA2308, an additional vehicle-anchored (VA) lap belt was used as shown in Figure 48.

Table 3. Dynamic frontal test matrix.

<b>ID</b>	<b>Wheelchair</b>	<b>Prior test</b>	<b>Abbrev.</b>	<b>Restraint</b>
<b>WA2301</b>	Surrogate Wheelchair Base	NA	SWCB	WA_Lap
<b>WA2302</b>	KiMobility Catalyst 5	Static	KMC5_S	WA_Lap
<b>WA2303</b>	KiMobility Catalyst 5	None	KMC5_0	WA_Lap
<b>WA2304</b>	TiLite ZRA	Static	TLZ_S	WA_Lap+VA_Lap
<b>WA2305</b>	Convaid Safari SFT 810	None	CVS_0	WA_Lap+VA_Lap
<b>WA2306</b>	KiMobility Catalyst 5	Aircraft Frontal, replaced front casters	KMC5*_AF	WA_Lap+VA_Lap
<b>WA2307</b>	Pride Mobility 3	Dynamic Frontal	PM3_DF	VA_Lap
<b>WA2308</b>	Quantum Q6 Edge 2	Dynamic Lateral	QE2_DL	WA_Lap+VA_Lap

*WA = wheelchair anchored, VA = vehicle anchored*



Figure 48. Example of ATD secured by both wheelchair-anchored lap belt and vehicle-anchored lap belt.

## Results

The first two tests (two test of the same model wheelchair) did not meet requirements, as the left front caster wheel broke in each test. Overall, results were similar between the two chairs, indicating that prior successful static testing did not seem to affect dynamic performance. The remaining frontal dynamic tests were conducted using an additional vehicle-attached lap belt and none of the wheelchairs experienced any structural failures.

In the first two commercial tests performed with the Ki Mobility Catalyst 5, one previously tested statically and the second not previously tested, the front left caster wheel broke off late in the event. In the first test, the left footrest also detached. Figure 49 shows images of how the damage occurred over the test. Since these WC19 wheelchairs did not have caster failure during WC19 certification testing, we identified several contributing factors. The restraint by only a lap belt and no shoulder belt, coupled with the orientation 10 degrees from frontal, allows the ATD head to rotate and hit left leg, transferring force into caster.

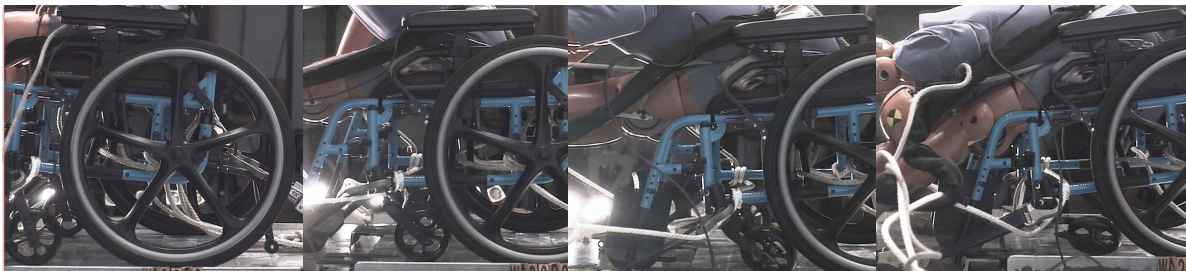


Figure 49. Sequence of closeup images from left video showing fracture of left front caster wheel.

We also wondered whether the steeper UMTRI pulse contributed, even though the failure happens late in the event. Because we had available a FEM of the KMC5 developed in a previous study, we conducted simulations using the UMTRI and triangular FAA pulses to examine the strain levels at the point of failure. An illustration of peak strain for each condition is shown in Figure 50. The maximum strain occurred in the same element for each simulation, and the values were similar (0.199 for UMTRI, 0.216 for triangular) although the peak values occurred at 120 ms for UMTRI and at 165 ms for triangular.

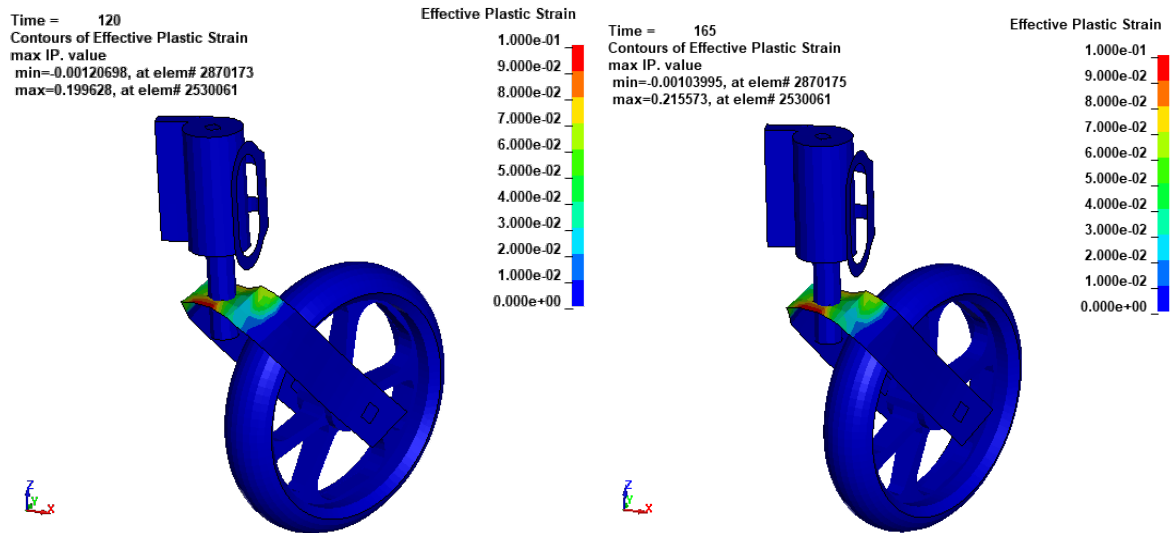


Figure 50. FEM results with KMC5 showing effective plastic strain distribution under UMTRI (left) and FAA (right) pulses.

For the subsequent dynamic frontal testing plots included in this report, blue lines are tests with the KMC5, black with the TLZ, gray with the CVS, orange PM3, and red QE2. Thicker lines represent tests run with only a wheelchair-attached lap belt, while thinner lines include use of a vehicle-attached lap belt. The suffixes in the legend indicate whether the wheelchair had been tested previously. Types of prior testing are static aircraft (S), none (0), dynamic WC19 or ISO 19 frontal tests (DF), dynamic lateral (DL), or dynamic aircraft with casters replaced (AF).



Figure 51 shows an overlap plot of the sled acceleration, while Figure 52 shows the integrated sled velocity. All tests achieved the target peak acceleration of 16 g (within 0.2 g) and the targeted minimum change in velocity of 48.2 km/hr. As noted previously, our rise time of approximately 10 ms is steeper than the maximum allowed time to peak of 90 ms.

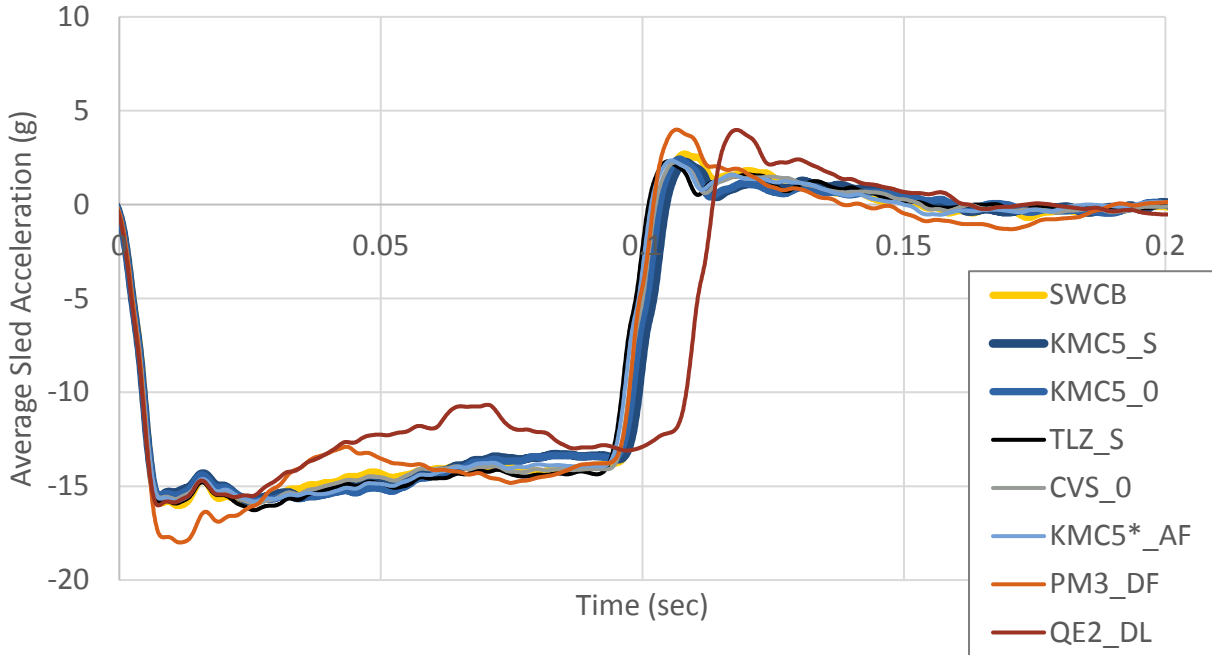


Figure 51. Average sled accelerations from all tests.

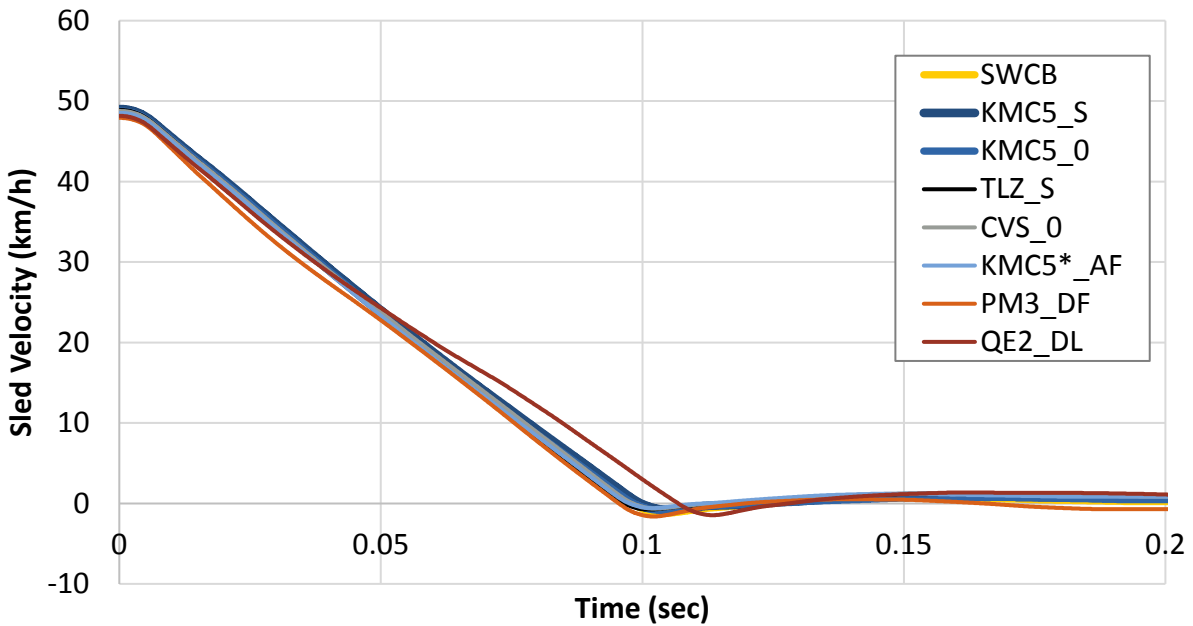


Figure 52. Sled change in velocity from all tests.

Figure 53 shows the lap belt loads from the frontal dynamic tests. In Figure 53, the solid lines show the load from the wheelchair-attached lap belt, while the dashed lines show the loads from the vehicle-mounted lap belt. Using the vehicle-mounted lap belt substantially decreased the loads in the wheelchair-mounted lap belt. Since PM3 is certified to ISO 7176-19 rather than WC-19, it did not have the option for a wheelchair-mounted lap belt and was only tested with the vehicle-mounted lap belt.

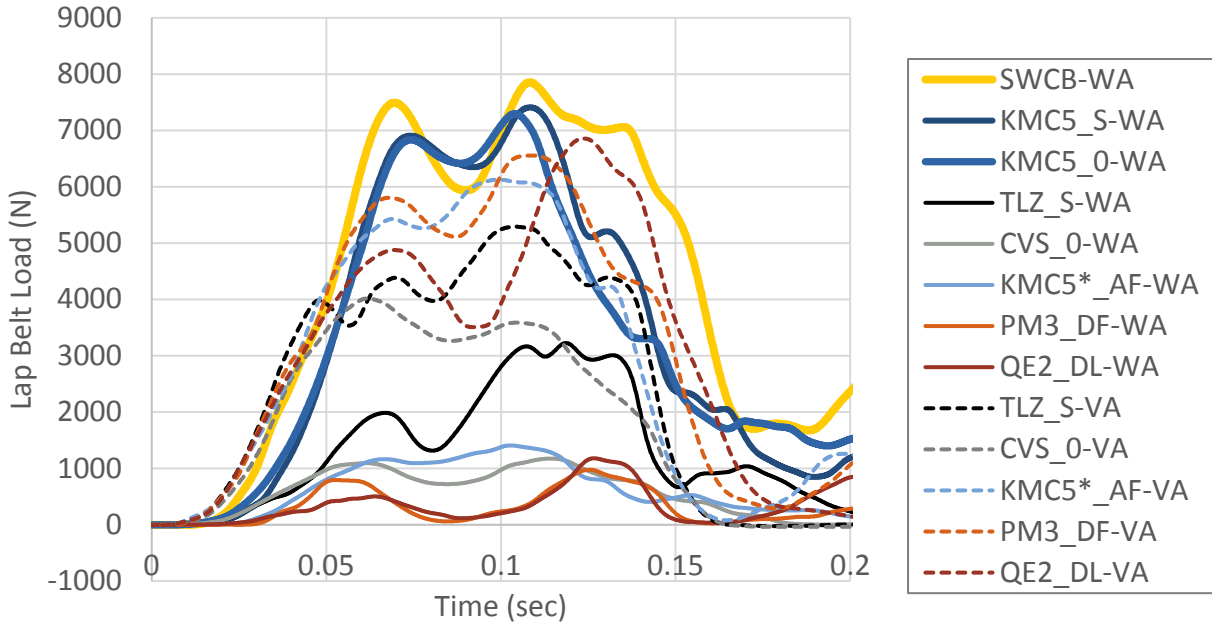


Figure 53. Lap belt load from all frontal tests.

Figure 54 shows the rear tiedown loads. On this plot, solid lines are the left rear tiedown and dashed lines are the right rear tiedown. Data are missing for the QE2 right tiedown because of instrumentation problems. The tiedown loads under aircraft testing are similar in magnitude to the range seen in WC19 testing. The peak right tiedown load is generally somewhat larger than the left tiedown load because of the 10-degree yaw angle relative to the frontal direction of travel.

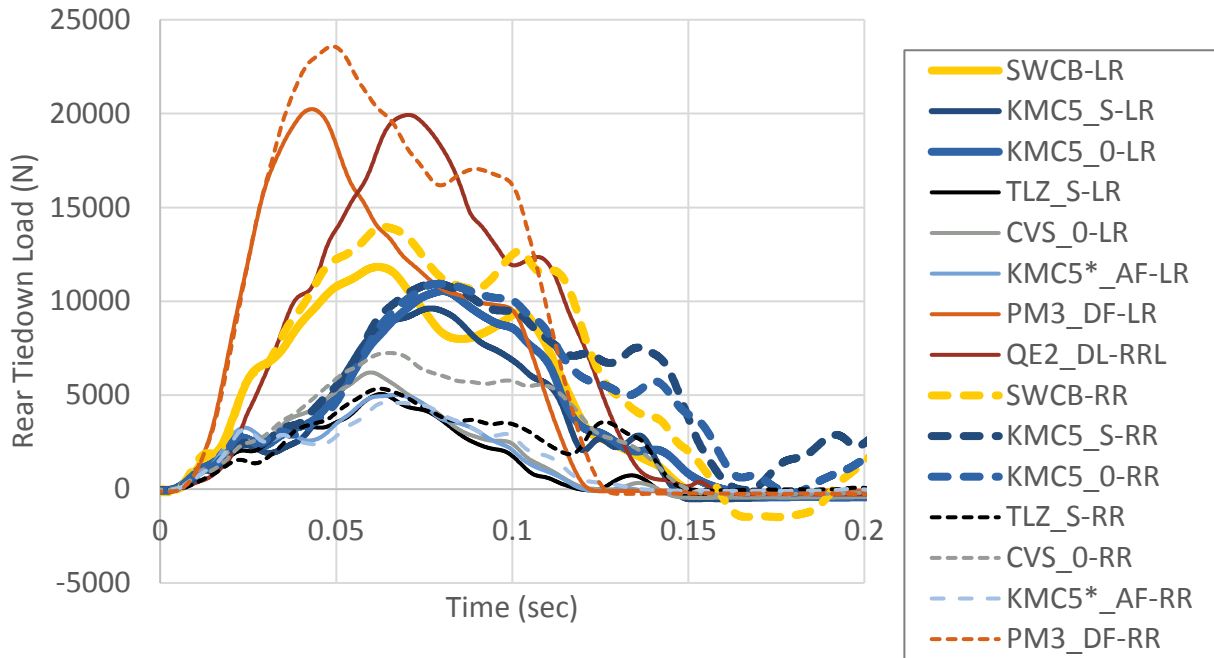


Figure 54. Rear tiedown loads from all frontal tests.

Figure 55 shows the head resultant acceleration from the dynamic frontal tests, truncating each channel just prior to the main head-to-leg contact. HIC is only calculated when ATD head contact occurs with something other than the ATD.

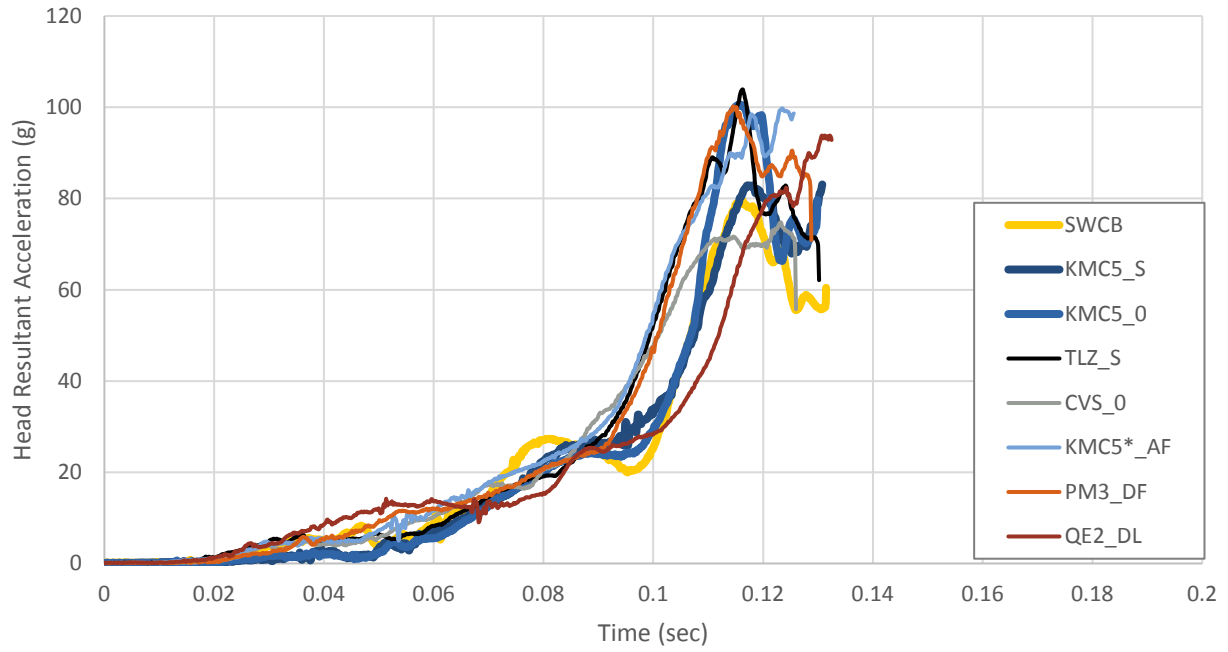


Figure 55. Head resultant acceleration prior to head-to-leg contact from all frontal tests.

The axial lumbar forces from the dynamic frontal tests are shown in Figure 56. All tests resulted in tensile loading of the lumbar spine.

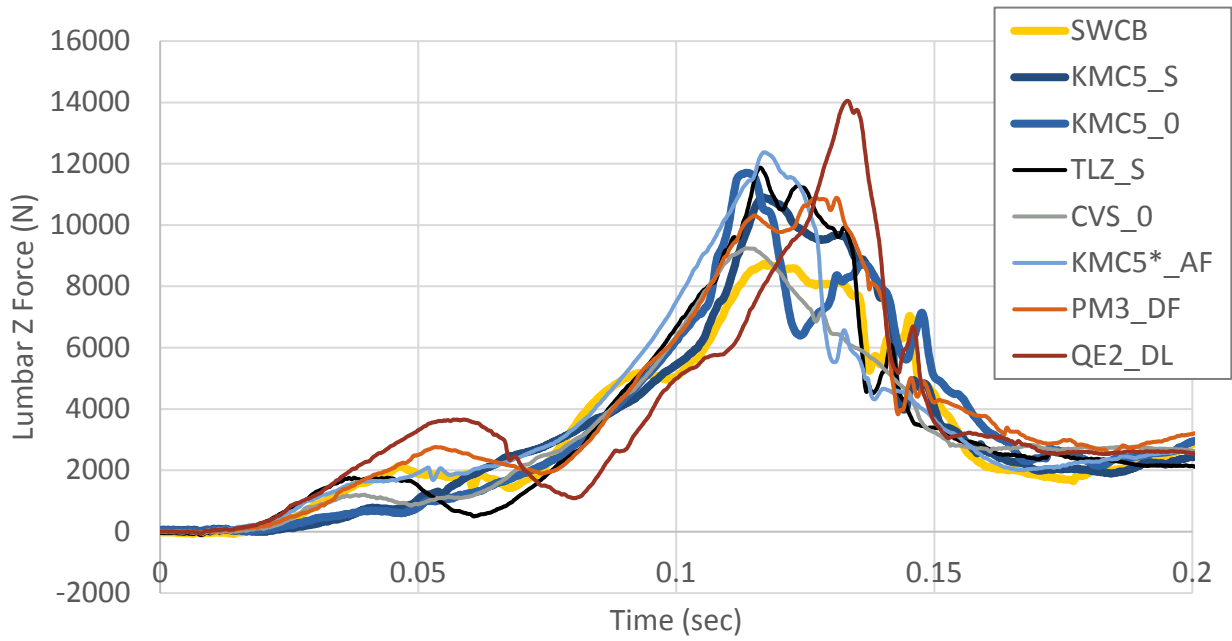


Figure 56. Lumbar axial force from all frontal tests.

Head trajectories digitized from the head CG target in each test are shown in Figure 57, with the origin at the WC seat/seatback junction. A line representing a 107 cm (42 in) bulkhead is included for reference. Generally, the tests with the additional vehicle-anchored lap belt had lower excursions than those without. All tests with the commercial wheelchairs had head CG trajectories of less than 900 mm relative to the SRP, indicating that head contact with a bulkhead positioned at 107 cm (42 in) would be unlikely.

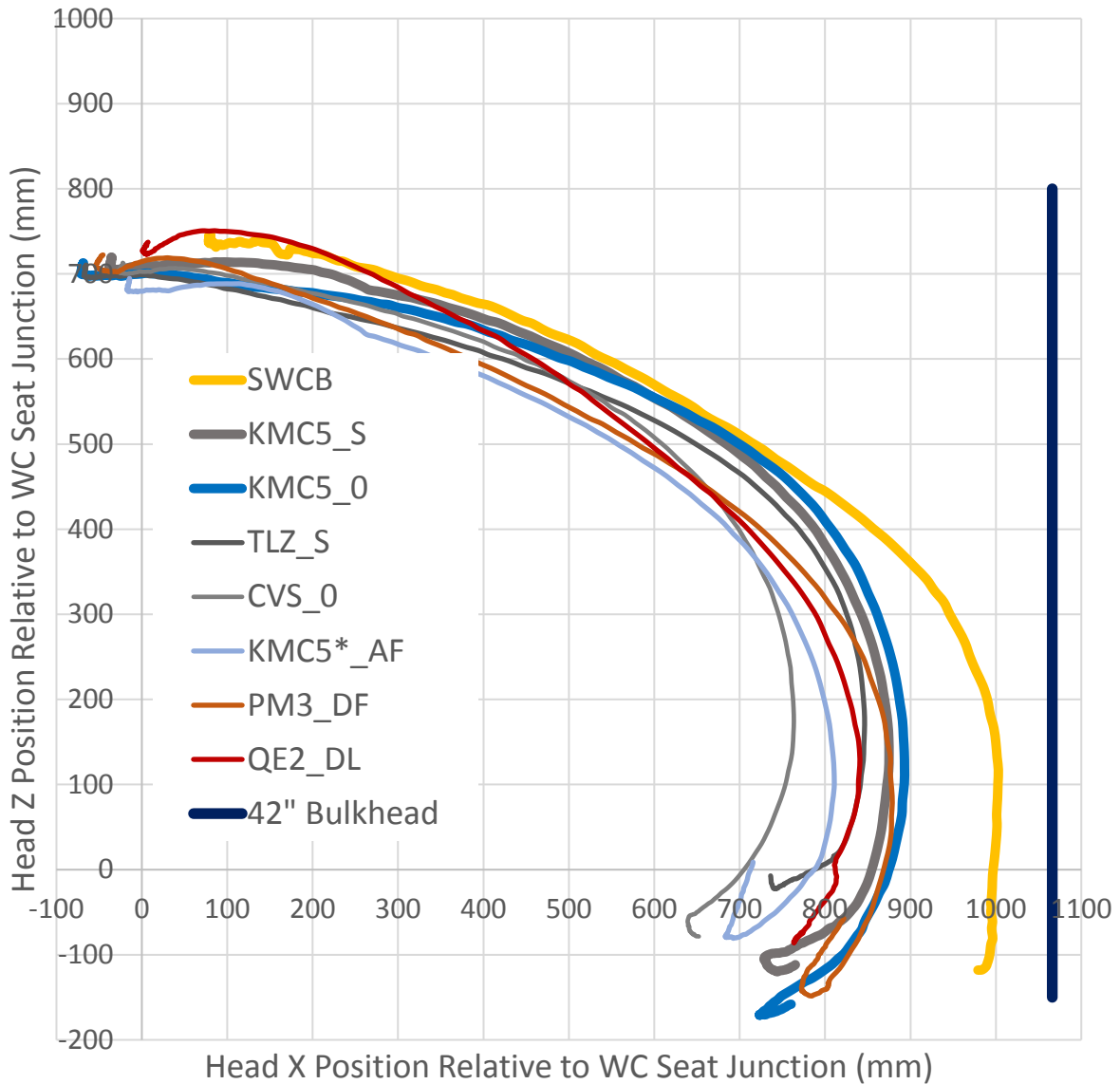


Figure 57. ATD head path relative to the wheelchair seat junction from all frontal tests.

FAA assessment measures are limited to maximum compressive lumbar force, as well as strap loads, femur force, and HIC when there is a forward bulkhead representation. However, we collected additional data on the chest, pelvis, and neck response that are included in Appendix A. Example kinematics for the CVS are shown in Figure 58 and Figure 59.

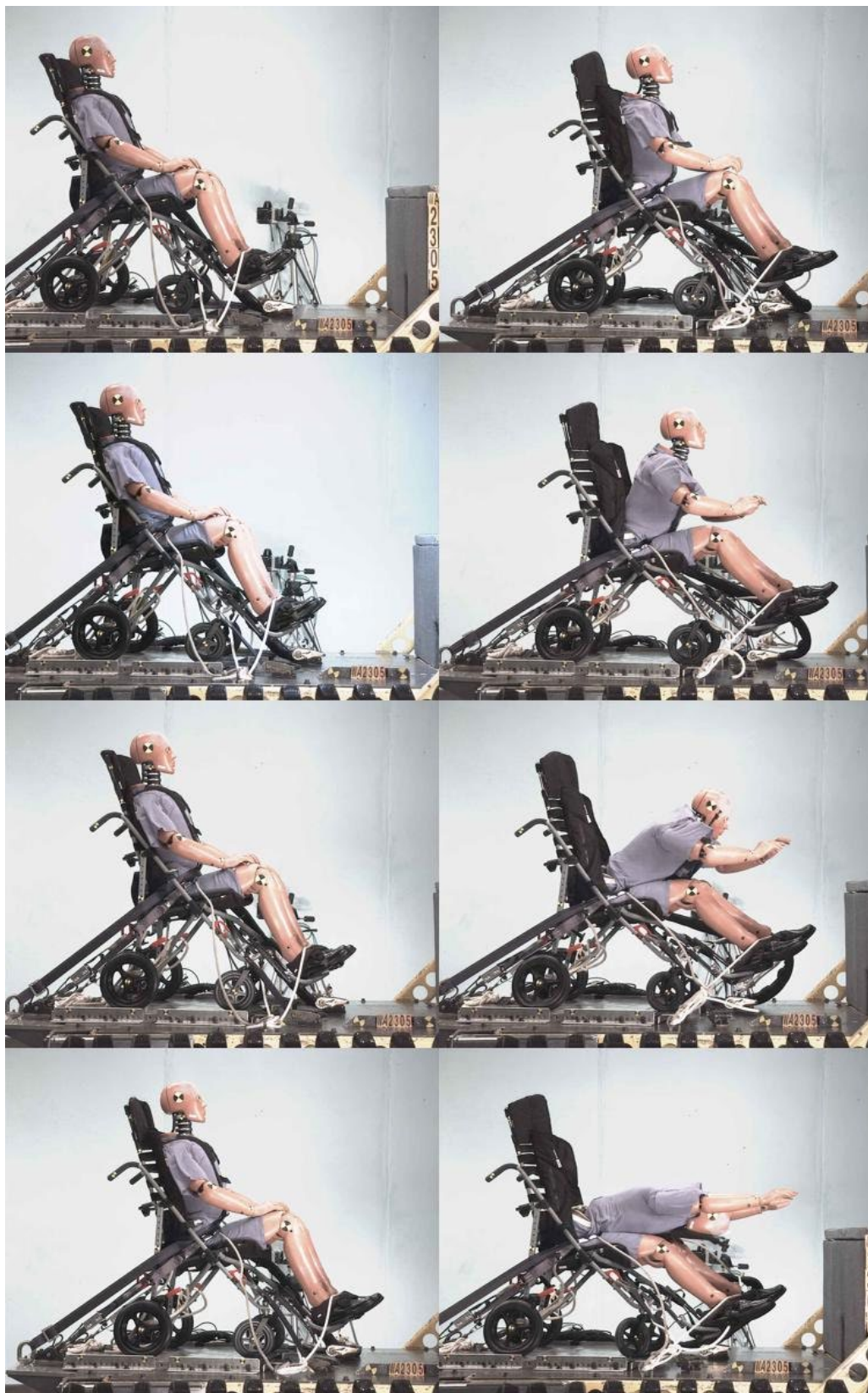


Figure 58. Example sideview kinematics under frontal dynamic loading for CVS\_0.



Figure 59. Example overhead kinematics under frontal dynamic loading for CVS\_0.



## Discussion

In all of our tests adapting FAA aircraft seating procedures to evaluate wheelchairs, we secured the wheelchairs using surrogate 4-point strap tiedowns using the geometry specified for testing in WC19. We chose this tiedown configuration because it would load the wheelchair's securement brackets in a similar manner for which it was designed. This geometry aims to have the rear tiedown strap angle oriented between 45 - 30 degrees, with the rear tiedowns placed straight back from the securement points and the front tiedowns placed forward and outboard of the front securement points for increased lateral stability. Should WC19 wheelchairs be allowed for use as seating on aircraft, we would recommend a similar configuration of anchor hardware for wheelchair stations on aircraft, to avoid needing to conduct additional testing using alternative tiedown anchor geometry. While the recommended configuration could have potential to impede egress for any passengers located outboard of the wheelchair station, this tiedown configuration is recommended and regularly used on public and school buses. Strategies from these configurations could provide insight on how to implement wheelchair stations with similar geometry on aircraft. In addition, simulations conducted with the recommended anchor geometry compared to a system that anchors directly below the securement points shows that increased head excursion and floor loads would occur with more compact tiedown geometries.

For the static testing, we followed a strict interpretation of the procedures, where we measured the mass of the entire wheelchair, added the occupant mass, and multiplied by the specified scaling factor for each direction. All the load was directed through the body block fixture and wheelchair-mounted lap belt. The manual wheelchairs were able to meet the requirements, but the power wheelchairs all experienced failure in the lateral and frontal directions. Since the heaviest wheelchair was almost 400 lb, this meant we were aiming to apply nearly 5000 lb of load in the frontal static test. A limitation of our static test setup is that the loading onset rate from our winch controller was faster and perhaps more extreme than the rate used by FAA.

Discussions with FAA experts indicated that aircraft seat manufacturers typically draft a test plan stating how they interpret the test procedures based on the characteristics of the seats they are testing, which can vary depending how they are mounted to the aircraft. FAA policy experts suggested that for power wheelchairs, it would be a reasonable interpretation to split the load into two parts. The pull force associated with weight of the seat and occupant would be directed through the body block, while the pull force associated with the weight of the wheelchair base would be directed through the front tiedown anchors. In addition, because the additional vehicle-mounted lap belt was required for wheelchairs to pass the frontal dynamic testing, static tests should also be conducted with the secondary lap belt. Future static testing will implement these recommendations and a slower onset rate with better control, and a draft of the specific test plan for each wheelchair will be submitted to FAA for review before proceeding.

Our original test plan for this project called for first testing wheelchairs under the static loading conditions, then performing dynamic testing on the same wheelchairs. After the failures of the three power wheelchairs under static testing, we had concerns whether the prior static testing might weaken the wheelchairs to the point where they would not pass the dynamic testing. Comparison of tests WA2302 and WA2303 on the same KMC5 wheelchair with and without prior static testing and similar results in terms of ATD signals and similar front left caster

failures did not support this concern. For future testing of power wheelchairs, we plan to conduct the dynamic tests before conducting the static tests.

Our initial plan to quantify deformations using 3D scans before and after each test did not produce results we have confidence in, as the scans were conducted off of the sled, making it difficult to align them sufficiently to allow calculations. For future testing we will scan the wheelchairs when they are secured to the sled by the tiedowns before and after each test. In addition, we will work with FAA to identify landmarks of interest to document with the FARO arm 3D measurement tool, so they are analogous to points measured on aircraft seats to evaluate residual deformation.

A limitation of this study is that the UMTRI sled pulse is trapezoidal, and cannot be used to generate the ideal triangular-shaped pulse. While our frontal pulse meets all the legal requirements of 14 CFR 25 in terms of achieving the peak acceleration and change in velocity within 90 ms, it achieves them sooner than is required. Thus, the UMTRI version of the FAA pulse is somewhat more severe than is needed. Simulations estimated that ATD kinematics would be similar in magnitude but happen earlier. Peak ATD measures and forces between the wheelchair, ATD, and floor are 13-18% higher with the UMTRI FAA pulse compared to the triangular FAA pulse. Comparing these measures by evaluating the area under the curves shows that those generated by the UMTRI FAA pulse have 2-11% greater area under the curve. This means that wheelchairs passing dynamic FAA requirements at UMTRI will likely have no issues passing dynamic tests using the triangular FAA pulse.

For the dynamic frontal testing, wheelchairs were able to pass when the ATD was restrained by an additional vehicle-anchored lap belt, in addition to the wheelchair-anchored lap belt available on WC19 products. As shown by the lap belt loads in Figure 53, adding the vehicle-mounted lap belt substantially reduced the loads carried by the wheelchair-mounted lap belt. This strategy was suggested by an FAA expert observing the tests. Because of concerns about how difficult it might be to determine whether an aircraft passenger's wheelchair actually was equipped with a crashworthy lap belt, the FAA had been considering requiring use of an aircraft-mounted lap belt as backup. Since the extra vehicle-mounted lap belt seemed to allow the wheelchairs tested to meet the frontal testing requirements, all future evaluation of wheelchairs for potential use as aircraft seating should incorporate use of the extra vehicle-mounted lap belt. Test WA2307 involved testing of a wheelchair previously tested to ISO 7176-19 standards; it did not have the option for a wheelchair-anchored lap belt. It did pass the FAA requirements, suggesting that the vehicle-mounted lap belt option may facilitate use of ISO certified wheelchairs. However, additional testing of more products would be needed to confirm this preliminary result because WC19 wheelchairs experience more load during frontal impact testing than ISO compliant wheelchairs.

The SWCB was developed to take the place of commercial wheelchair frames when assessing different seating systems. We primarily chose to use it during FAA testing, rather than the SWC, because the static body block would not fit in between the fixed armrest of the SWC. All tests were first conducted using the SWCB to identify procedural issues before conducting tests on commercial products. The response of the SWCB in frontal dynamic testing conditions was within the range of commercial products.

For the frontal dynamic testing, we did not simulate the pitch and roll typically used to represent floor deformation during testing of wheelchair. The intent of this requirement is to show that aircraft seats rigidly secured to the aircraft floor remain in place should the floor deform in a crash. For wheelchairs secured by 4-point tiedown straps that include webbing, the tensions among the four tiedowns would shift under floor deformation but would not be expected to fail. Simulations of the frontal dynamic test with and without floor deformation confirmed this expectation.

This study evaluated wheelchairs meeting WC19 requirements for ground vehicles as potential seats on aircraft. While preliminary results are promising, a challenge is that most people currently do not use WC19 wheelchairs. In an ongoing study of wheelchair geometry being performed by the UMTRI team, only one of 80 volunteers was using a WC19 wheelchair. Wheelchairs are regulated as medical devices by the FDA, which does not require wheelchairs to be crashworthy for use as vehicle seating. NHTSA does not address wheelchairs used as vehicle seats. While the cost of adding WC19 hardware is \$200 to \$500 on wheelchairs that can cost \$1500 to \$20,000, the cost is not currently covered by most insurers, with the exception of the Veterans Administration. As a result of this and also concerns about product liability, most wheelchair manufacturers do not promote the availability of the WC19 option. It may be possible to retrofit some wheelchair models with hardware, but most insurers cover wheelchair replacement every five years, and many users would not be able to cover the out-of-pocket costs to add the WC19 option themselves.

## **Summary and Conclusions**

This project focuses on the impact response of WC19-compliant wheelchairs tested under the static and dynamic tests required for aircraft seating. Observations to date include:

- Computer simulations of frontal testing showed minimal differences with and without floor deformation when the wheelchair is secured by 4-point strap tiedowns, so floor deformation was not evaluated during physical testing.
- Computer simulations showed that the UMTRI version of the FAA pulse provides similar kinematic response to the triangular pulse.
- Two manual wheelchairs were able to pass a simple interpretation of static loading requirements.
- Three power wheelchairs failed a simple interpretation of static loading requirements, but FAA policy experts suggested an alternative strategy that will be investigated in the next year.
- Five WC19 wheelchair models (two power, three manual) were able to pass frontal dynamic testing requirements when a vehicle-mounted lap belt was used in addition to the wheelchair-mounted lap belt.

## **Ongoing Work**

Continuing work in the current project to evaluate wheelchairs as potential aircraft seating will include the following tasks:

- Improving the controller and mechanism used for conducting static tests.
- Designing and building fixtures to allow testing of wheelchairs to the vertical FAA test condition, with the simulated floor oriented at 60 degrees relative to horizontal.
- Drafting a revised interpretation of the test procedure for conducting static testing of power wheelchairs that allocates load between the body fixture and the wheelchair tiedown securement points.
- Identifying landmarks on wheelchairs and improved methods to allow appropriate evaluation of residual deformation.
- Conducting additional static testing and vertical dynamic testing using a combination of wheelchair- and vehicle-mounted lap belts.

## Bibliography

- [1] W. Erickson, C. Lee, and S. von Schrader, “2017 Disability Statistics Report,” [https://disabilitycompendium.org/sites/default/files/user-uploads/2017\\_AnnualReport\\_2017\\_FINAL.pdf](https://disabilitycompendium.org/sites/default/files/user-uploads/2017_AnnualReport_2017_FINAL.pdf), 2018, [Online]. Available: [https://disabilitycompendium.org/sites/default/files/user-uploads/2017\\_AnnualReport\\_2017\\_FINAL.pdf](https://disabilitycompendium.org/sites/default/files/user-uploads/2017_AnnualReport_2017_FINAL.pdf)
- [2] National Academies of Sciences, Engineering, and Medicine, “Technical Feasibility of a Wheelchair Securement Concept for Airline Travel,” Washington DC, USA, 2021. doi: 10.17226/26323.
- [3] B. Dawson, “A disability activist died from body sores associated with the loss of her \$30,000 wheelchair that was ‘destroyed’ during a United Airlines flight, advocacy group claims,” *Business Insider*, 2021. [Online]. Available: <https://www.businessinsider.com/disability-activist-died-after-united-airlines-destroyed-30k-wheelchair-2021-11>
- [4] Department of Justice, *Americans with Disabilities Act: Title III Regulations*. 2010.
- [5] Architectural and Transportation Barriers Compliance Board., *Americans With Disabilities Act (ADA) Accessibility Guidelines for Transportation Vehicles*. 2016. [Online]. Available: <https://www.access-board.gov/guidelines-and->
- [6] RESNA, *Wheelchair containment and occupant retention systems for use in large accessible transit vehicles : systems for rearward-facing passengers*. 2017, pp. 1–42.
- [7] RESNA, *Wheelchair tiedown and occupant restraint systems for use in motor vehicles*. 2017, pp. 1–93.
- [8] RESNA, *Wheelchairs Used as Seats in Motor Vehicles*. 2017, pp. 1–105.
- [9] RESNA, *Wheelchair Seating Systems for Use in Motor Vehicles*. 2017, pp. 1–58.
- [10] SAE, “Performance Standard for Seats in Civil Rotorcraft, Transport Aircraft, and General Aviation Aircraft (AS8049D),” 2020.
- [11] Federal Aviation Administration, “AC 25.562-1B - Dynamic Evaluation of Seat Restraint Systems and Occupant Protection on Transport Airplanes,” Sep. 2015.
- [12] G. E. Bertocci, M. A. Manary, and D. Ha, “Wheelchairs used as motor vehicle seats: Seat loading in frontal impact sled testing,” *Med Eng Phys*, vol. 23, no. 10, 2001, doi: 10.1016/S1350-4533(01)00102-3.
- [13] M. E. Buning *et al.*, “RESNA’s position on wheelchairs used as seats in motor vehicles,” *Assistive Technology*, vol. 24, no. 2, 2012, doi: 10.1080/10400435.2012.659328.
- [14] P. Karg *et al.*, “State of the science workshop on wheelchair transportation safety.,” *Assist Technol*, vol. 21, no. 3, pp. 115–160, 2009, doi: 10.1080/10400430903175663.

- [15] M. A. Manary, L. M. Woodruff, G. E. Bertocci, and L. W. Schneider, "Patterns of wheelchair response and seating-system failures in frontal-impact sled tests," *RESNA 26th Annual Conference Proceedings, Atlanta, GA*, 2003.
- [16] M. A. Manary, N. L. Ritchie, and L. W. Schneider, "WC19: A wheelchair transportation safety standard-Experience to date and future directions," *Med Eng Phys*, vol. 32, no. 3, pp. 263–271, Apr. 2010, doi: 10.1016/j.medengphy.2009.08.012.
- [17] N. L. Ritchie, M. A. Manary, G. E. Bertocci, and L. W. Schneider, "Validation of a surrogate wheelchair base for evaluation of wheelchair seating system crashworthiness," in *RESNA 29th Annual Conference*, Atlanta, GA, 2006. [Online]. Available: [http://www.ercwts.pitt.edu/RERC\\_WTS2\\_KT/RERC\\_WTS2\\_KT\\_Pub/RERC\\_WTS\\_Pub\\_Doc/RERC\\_WTS\\_Pub\\_06/RE\\_S\\_RitchieN\\_Paper.pdf](http://www.ercwts.pitt.edu/RERC_WTS2_KT/RERC_WTS2_KT_Pub/RERC_WTS_Pub_Doc/RERC_WTS_Pub_06/RE_S_RitchieN_Paper.pdf)[http://www.ercwts.pitt.edu/RERC\\_WTS2\\_KT/RERC\\_WTS2\\_KT\\_Pub/RERC\\_WTS\\_Pub\\_Doc/RERC\\_WTS\\_Pub\\_06/RE\\_S\\_RitchieN\\_Paper.pdf](http://www.ercwts.pitt.edu/RERC_WTS2_KT/RERC_WTS2_KT_Pub/RERC_WTS_Pub_Doc/RERC_WTS_Pub_06/RE_S_RitchieN_Paper.pdf)
- [18] N. L. Ritchie, M. A. Manary, L. van Roosmalen, and L. W. Schneider, "The Role of Armrest Design on Positioning of Belt Restraints on Wheelchair-Seated Drivers," *32nd RESNA Annual Conference Proceedings, New Orleans, LA*, 2009, [Online]. Available: [https://www.resna.org/sites/default/files/legacy/conference/proceedings/2009/Wheeled\\_Mobility/Ritchie.html](https://www.resna.org/sites/default/files/legacy/conference/proceedings/2009/Wheeled_Mobility/Ritchie.html)
- [19] M. A. Manary, N. L. Ritchie, C. A. C. Flannagan, G. E. Bertocci, and L. W. Schneider, "The effects of pelvic belt anchoring location on wheelchair seating system loads in frontal impact motor vehicle crashes," in *RESNA 32nd Annual Conference Proceedings, New Orleans, LA*, New Orleans, LA, 2009. [Online]. Available: [https://www.resna.org/sites/default/files/legacy/conference/proceedings/2009/Wheeled\\_Mobility/Manary.html](https://www.resna.org/sites/default/files/legacy/conference/proceedings/2009/Wheeled_Mobility/Manary.html)
- [20] L. W. Schneider, M. A. Manary, D. A. Hobson, and G. E. Bertocci, "Transportation Safety Standards for Wheelchair Users: A Review of Voluntary Standards for Improved Safety, Usability, and Independence of Wheelchair-Seated Travelers," *Assistive Technology*, vol. 20, no. 4, 2008, doi: 10.1080/10400435.2008.10131948.
- [21] L. W. Schneider and M. A. Manary, "Wheeled mobility tiedown systems and occupant restraints for safety and crash protection," in *Driver Rehabilitation and Community Mobility*, Mosby Inc., St. Louis, MO, 2006, pp. 357–372. doi: 10.1016/B978-032302937-7.50023-X.
- [22] N. L. Ritchie, M. A. Manary, G. E. Bertocci, and L. W. Schneider, "Validation of a surrogate wheelchair base for evaluation of wheelchair seating system crashworthiness," in *RESNA 29th Annual Conference Proceedings, Atlanta, GA*, Atlanta, GA, 2006. [Online]. Available: <https://www.resna.org/sites/default/files/legacy/conference/proceedings/2006/Research/Seating/Ritchie.html>
- [23] D. A. Hobson and L. van Roosmalen, "Towards the next generation of wheelchair securement—development of a demonstration udig-compatible wheelchair docking

- device,” *Assistive Technology*, vol. 19, no. 4, pp. 210–222, Dec. 2007, doi: 10.1080/10400435.2007.10131878.
- [24] M. J. Turkovich, L. van Roosmalen, D. A. Hobson, and E. A. Porach, “The effect of city bus maneuvers on wheelchair movement,” *J Public Trans*, vol. 14, no. 3, 2011, doi: 10.5038/2375-0901.14.3.8.
- [25] L. van Roosmalen, P. Karg, D. A. Hobson, M. J. Turkovich, and E. Porach, “User evaluation of three wheelchair securement systems in large accessible transit vehicles,” *The Journal of Rehabilitation Research and Development*, vol. 48, no. 7, p. 823, 2011, doi: 10.1682/JRRD.2010.07.0126.
- [26] L. Van Roosmalen, G. E. Bertocci, D. A. Hobson, and P. Karg, “Preliminary evaluation of wheelchair occupant restraint system usage in motor vehicles,” *J Rehabil Res Dev*, vol. 39, no. 1, 2002.
- [27] K. D. Klinich, N. R. Orton, J. Fischer, and M. A. Manary, “Volunteer Evaluation of Wheelchair Accessibility in Vehicles,” 2022. Accessed: Dec. 07, 2022. [Online]. Available: <https://deepblue.lib.umich.edu/handle/2027.42/174701>
- [28] K. D. Klinich, N. R. Orton, J. Fischer, and M. A. Manary, “Volunteer Evaluation of Wheelchair Accessibility in Vehicles,” 2022. Accessed: Dec. 07, 2022. [Online]. Available: <https://deepblue.lib.umich.edu/handle/2027.42/174701>
- [29] K. D. Klinich, N. R. Orton, M. A. Manary, E. McCurry, and T. Lanigan, “Independent Safety for Wheelchair Users in Automated Vehicles,” Ann Arbor, MI, 2022.
- [30] K. D. Klinich, N. Orton, L. Malik, E. Zak, M. St. Amour, and M. Manary, “Volunteer Evaluation of an Automated Wheelchair Tiedown and Occupant Restraint System,” 2021.
- [31] K. D. Klinich, M. A. Manary, K. J. Boyle, N. R. Orton, and J. Hu, “Development of an Automated Tiedown and Occupant Restraint System for Automated Vehicle Use,” 2021.
- [32] United States Access Board, *PART 1192 — AMERICANS WITH DIS- ABILITIES ACT ( ADA ) ACCESSIBIL- ITY GUIDELINES FOR TRANSPOR- Subpart A — General*. 1998, pp. 391–425.
- [33] United States Department of Justice, “2010 ADA Standards for Accessible Design,” 2010.
- [34] V. Gowdy *et al.*, “A lumbar spine modification to the hybrid III ATD for aircraft seat tests,” in *SAE Technical Papers*, SAE International, 1999. doi: 10.4271/1999-01-1609.
- [35] Philippens Mat MGM, Forbes Patrick A, Wismans Jac SHM, DeWeese Rick, and Moorcroft David, “Neck Injury Criteria for Side-Facing Aircraft Seats,” 2011.

## **Appendix A. Additional Dynamic Testing Results**



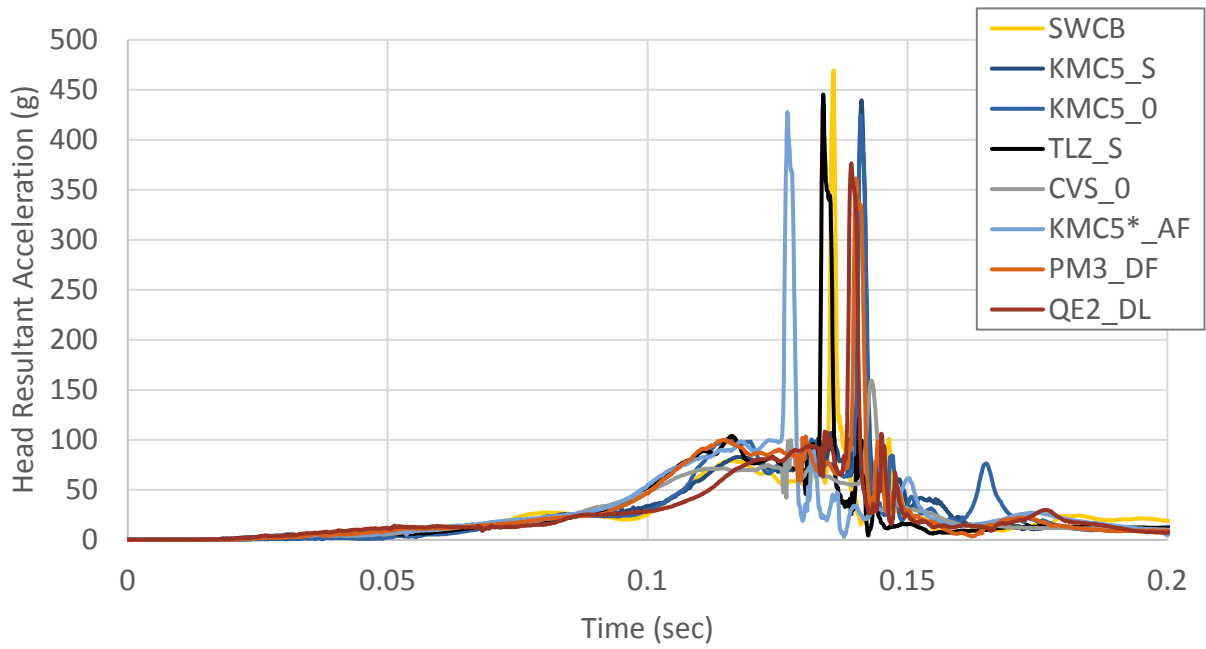


Figure 60. Complete head resultant acceleration from all frontal tests.

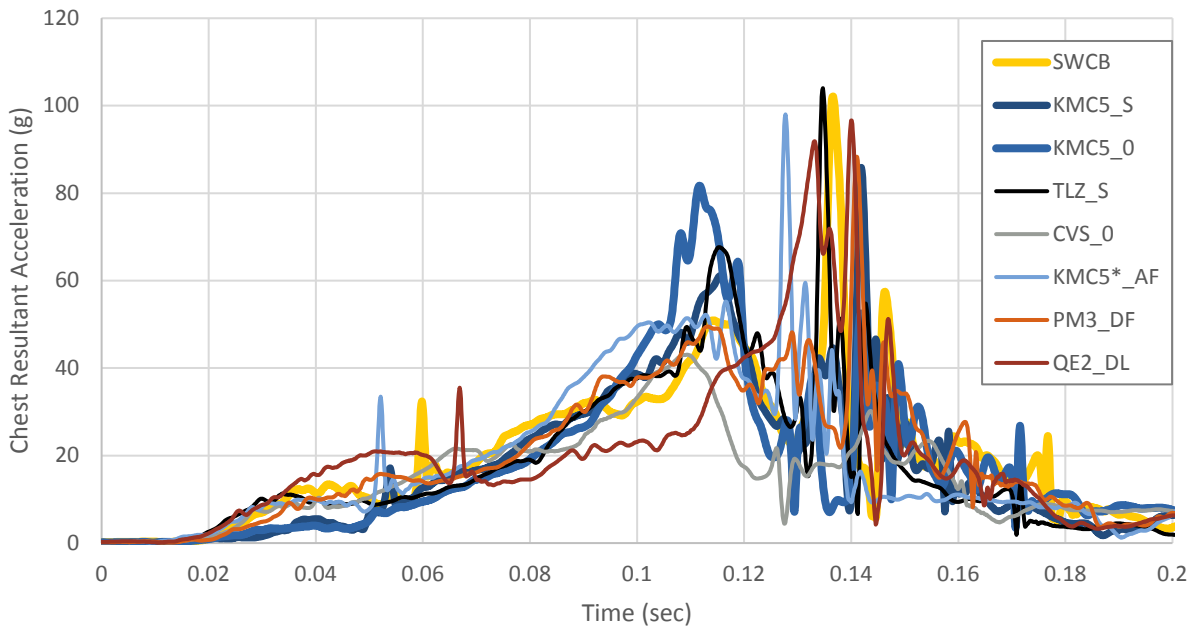


Figure 61. Chest resultant acceleration from all frontal tests.

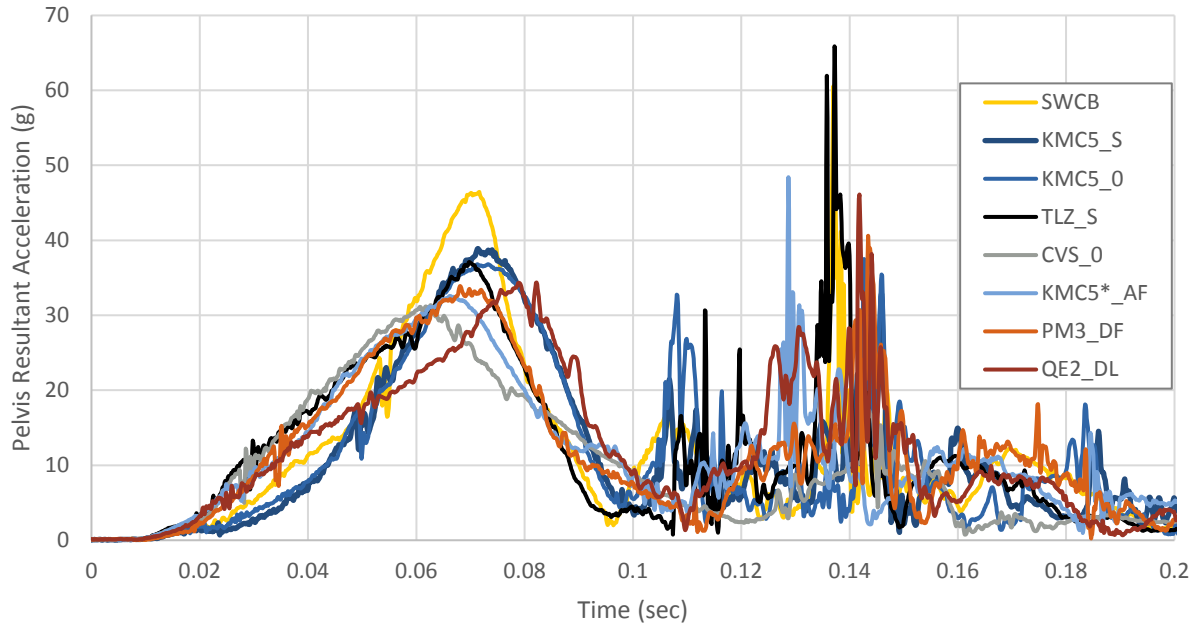


Figure 62. Pelvis resultant acceleration from all frontal tests.

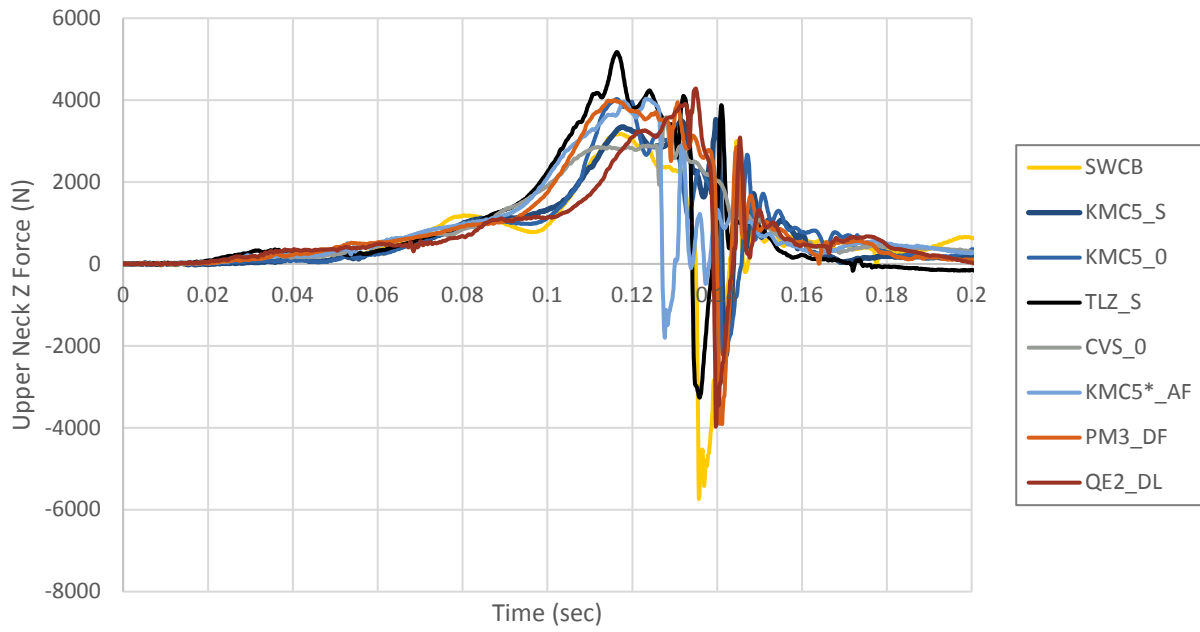


Figure 63. Upper neck axial force from all frontal tests.

## **Appendix B. Draft Test Procedure for Wheelchairs Under Frontal Aircraft Seating Conditions**

## **Introduction**

These procedures were developed to evaluate how to test wheelchairs according to FAA requirements for aircraft seating. The FAA requirements have been adapted for wheelchair testing using methods and requirements from RESNA WC-4:2017. For the frontal test procedure, the WC19 test bench is rotated 10 degrees clockwise or counterclockwise from the forward direction of travel.

## **Wheelchair Test Methods**

### *Equipment*

The equipment needed to conduct this testing includes:

- A complete commercial wheelchair that complies with ANSI/RESNA WC19.
- A dynamic sled with a flat rigid mounting surface capable of producing the 16-g, 48.2 km/hr test specified in 14 CFR 25
- Calibrated instrumentation to verify the tested pulse with a data collection system that complies with SAE J211
- A midsized male FAA Hybrid III ATD.
- A surrogate WTORS meeting the description of Annex D of ANSI/RESNA WC19.
- Three high speed digital video cameras capable of recording images at 1000 fps, placed right side perpendicular to sled travel, overall left side perpendicular to the WPS, and overhead

Prior to conducting the test, make sure the sled instrumentation has been calibrated per the manufacturer in the previous 12 months. Inspect the ATD for damage and adjust the joints to a resistance of 1 g. Clothe the ATD in snug fitting cotton clothing as specified in federal crash testing standards. Verify that the wheelchair is in good working order and the tires are inflated per manufacturer's specifications.

### *Test Procedures*

1. Define a wheelchair station on the sled platform that is at least 76 cm (30 in) wide and 123 (48 in) long.
2. Orient the centerline of the wheelchair station so that in the plan (overhead) view, the centerline of the station is rotated 10 degrees from the primary direction of sled travel.
3. The wheelchair should be adjusted to fit the ATD per the manufacturer's instructions and all adjustment mechanisms should be tightened per the user manual.
4. Adjustable elements of the seat (such as tilt and recline) should be in a middle position rather than at the end of adjustment travel.
5. The seat back support angle should be between 5 and 30 degrees from vertical when measured unloaded at the seatback centerline.
6. The seat pan angle should be between 5 and 30 degrees from horizontal when measured unloaded at the seat centerline.
7. Install the SWTORS so that the anchor points that are:
  - a. Symmetrically located with respect to the wheelchair center line (aka the wheelchair reference place).

- b. At least 48 inches apart from front to rear of the wheelchair.
  - c. Installed so that the rear anchorages are directly behind the wheelchair securement points and the rear tiedown straps are parallel to the wheelchair centerline when viewed from overhead.
  - d. Installed so that the front tiedown points are outboard of the front wheelchair securement points, but not further apart than 76 cm (30 in).
8. Secure the wheelchair with the SWTORS.
    - a. While maintaining the wheelchair reference plane within  $3^\circ$  of the centerline of the wheelchair station, adjust the fore/aft position of the wheelchair while tensioning the tiedown straps to between 100 N and 200 N (about 22 lbf and 44 lbf), to achieve a side-view projected angle of the rear tiedown straps of  $45^\circ \pm 3^\circ$  to the horizontal.
    - b. If a rear tiedown-strap angle in this range cannot be achieved with a tiedown-strap length of at least 495 mm (19.5 in.), adjust the length of the rear tiedown strap assemblies to between 495 mm and 508 mm (19.5 in. and 20 in.), and measure the resulting side-view projected angle of the rear tiedown straps.
  9. Place the ATD into the wheelchair making sure the ATD is seated symmetrically with the torso upright and the back and legs pushed into and in contact with the wheelchair back support and seat.
  10. Position the wheelchair-anchored seat belt on the ATD with the lap belt routed at the junction of the pelvis/thigh.
  11. Position a second vehicle-mounted lap belt using the rear tiedown anchors as securement points and tighten until snug.
  12. Add targets to the following landmarks on the wheelchair (TBD). Record the coordinates of each prior to testing.
  13. Measure and record the SWTORS anchorage locations, tiedown strap angles, seat belt angles, the wheelchair width at the seat rails, the ATD H-point height, wheelchair back support angle, and wheelchair seat pan angle.
  14. Conduct the sled test.
  15. Measure and record the same landmarks measured in step 12 after the test is complete.

### **Wheelchair Performance Criteria**

When tested according to the procedures in this document, the wheelchair should meet the following requirements:

1. The wheelchair securement point structural components shall not fail completely.
2. The wheelchair securement points shall not deform such that the hooks of the four-point, strap-type surrogate tiedown system cannot be disengaged and removed.
3. The wheelchair should be in an upright position at the end of the test.
4. The ATD should be in a seated posture in the wheelchair at the end of the test, with the ATD torso leaning less than  $45^\circ$  from the vertical when viewed from all directions.
5. No rigid components, parts, equipment, or accessories with a mass greater than 150 grams (5.3 oz) should detach from the wheelchair during the test.
6. Wheelchair components that could contact the occupant seated in a wheelchair or nearby occupants should not break or separate in a manner that produces sharp edges with a radius of less than 2 mm (0.08 in.).

7. Locking mechanisms of tilt seating systems shall not have structural components that completely fail during the test. Shifting of seating-system orientation from release or slipping of a friction clamp are allowed if the sideview angle of the seating surface does not rotate below horizontal.
8. At the end of the test, the average height of the left and right ATD H-points relative to the wheelchair ground plane shall not have decreased by more than 20% from the pre-test average height.
9. At the end of the test, the average wheelchair width, measured at the seat rails shall not have decreased by more than 20% from the pre-test width.
10. Seats and back supports shall not separate or detach from the wheelchair or wheelchair frame unless there is a backup at the same point that remains functional.
11. No webbing of the surrogate wheelchair tiedown and occupant restraint system (SWTORS) or commercial WTORS shall completely fail due to interaction with the wheelchair or its components during a test.
12. All securement hooks of the SWTORS or commercial tiedown shall remain attached to the wheelchair securement points throughout the test.
13. Wheelchair-anchored belt restraints shall not become detached at anchorages, disconnected at buckles, or show complete webbing failure.
14. Batteries of power wheelchairs or their surrogate replacement parts shall:
  - i) not move completely outside the wheelchair footprint,
  - ii) remain attached or tethered to the battery compartment throughout the test,  
and
  - iii) shall not contact the ATD